High-resolution simulations of the South Asian monsoon under changing climate

R. Krishnan
Centre for Climate Change Research (CCCR)
Indian Institute of Tropical Meteorology, Pune

Collaborators: T.P. Sabin, R. Vellore, M. Mujumdar, J. Sanjay, B.N.Goswami

J.-L. Dufresne, F. Hourdin, P. Terray; IITM-ESM Team

Advanced School on Earth System Modeling

IITM, Pune 18-27 July, 2016

The South Asian Monsoon

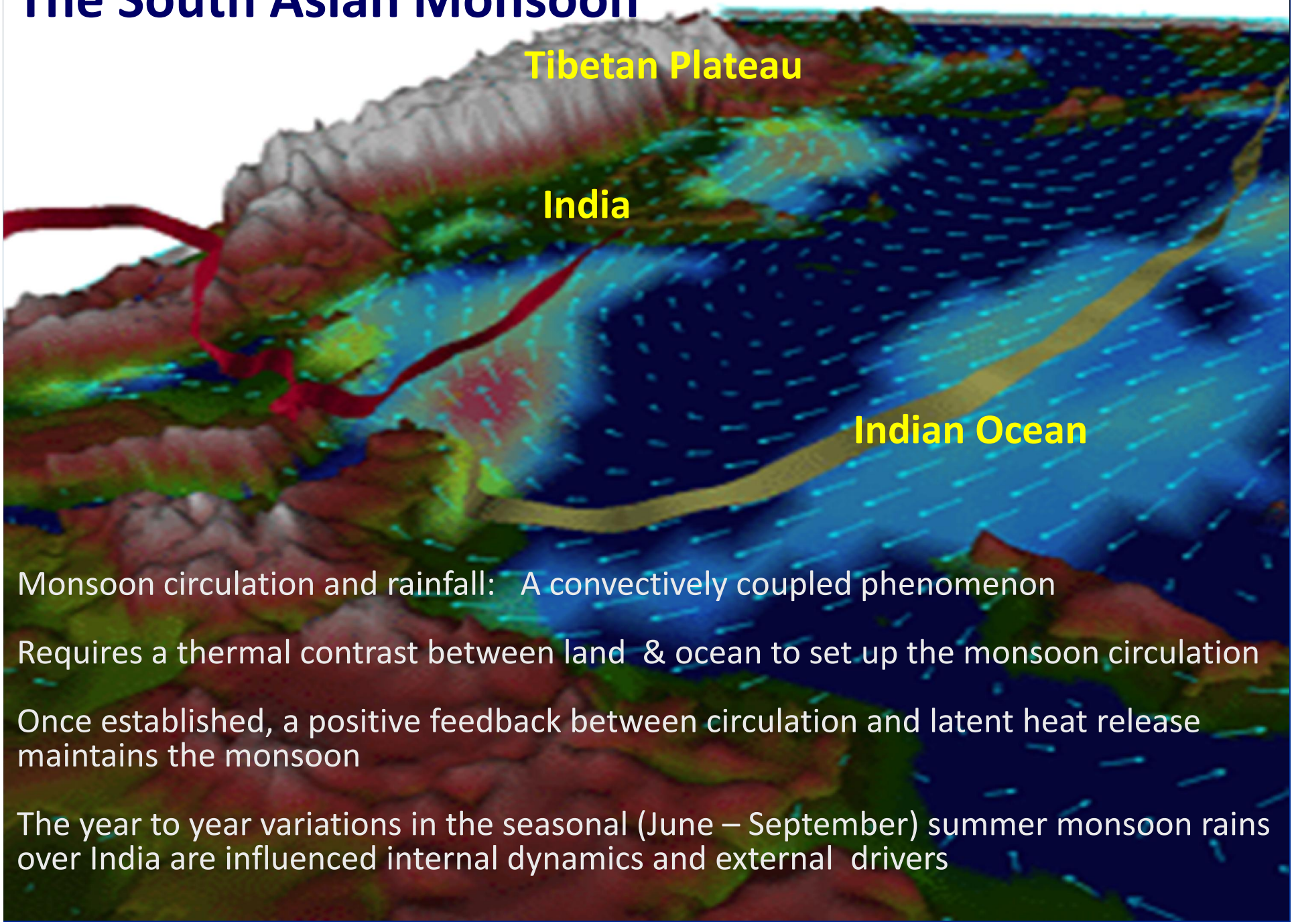

Monsoon circulation and rainfall: A convectively coupled phenomenon

Requires a thermal contrast between land & ocean to set up the monsoon circulation

Once established, a positive feedback between circulation and latent heat release maintains the monsoon

The year to year variations in the seasonal (June – September) summer monsoon rains over India are influenced internal dynamics and external drivers

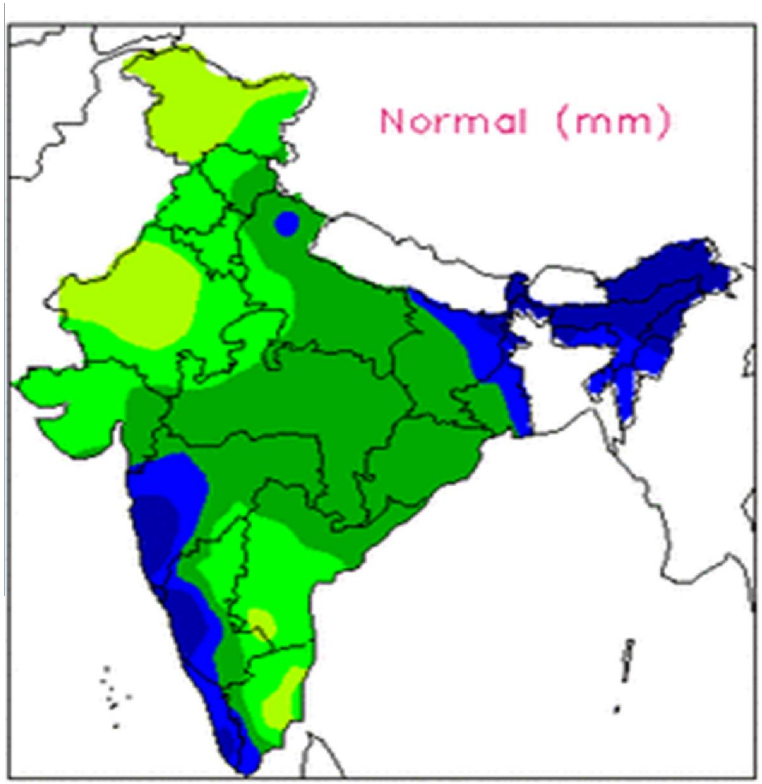

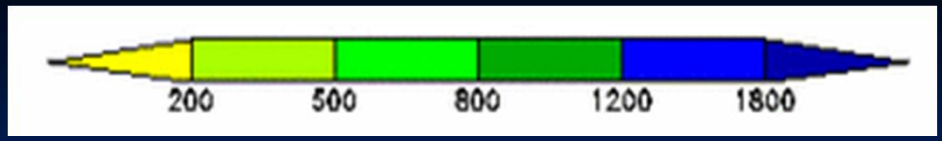

Long-term climatology of total rainfall over India during (1 Jun - 30 Sep) summer monsoon season (http://www.tropmet.res.in)

Interannual variability of the Indian Summer Monsoon Rainfall

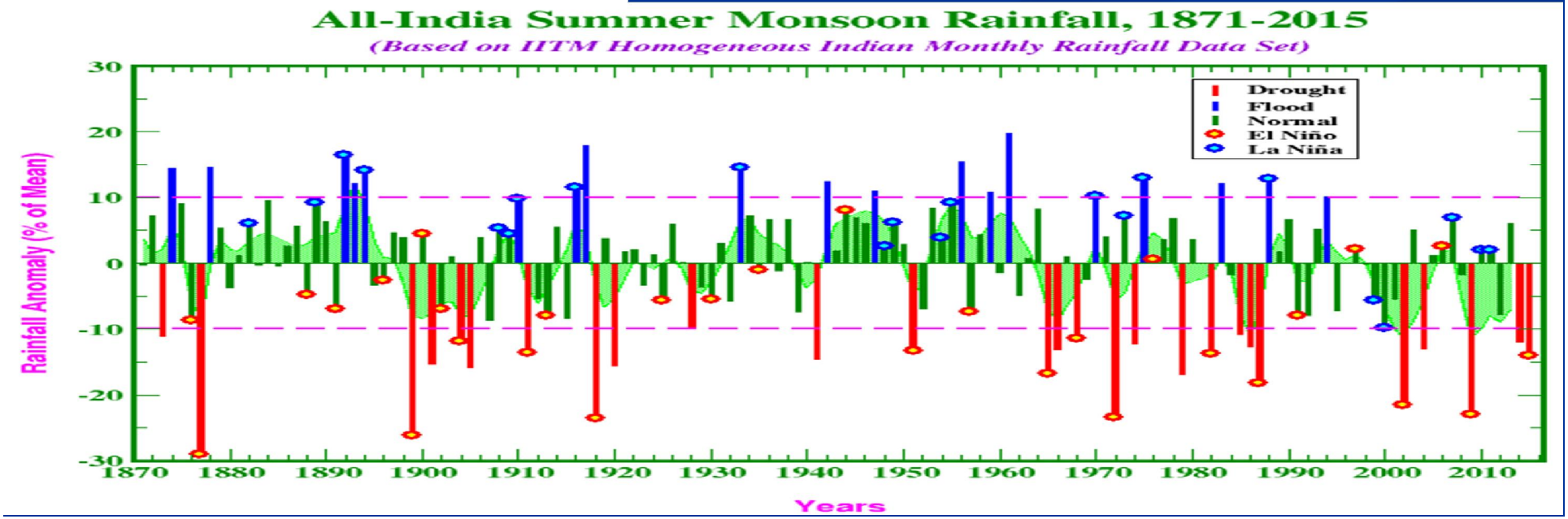

Spatial map of linear trend of JJAS rainfall (1951 – 2007)

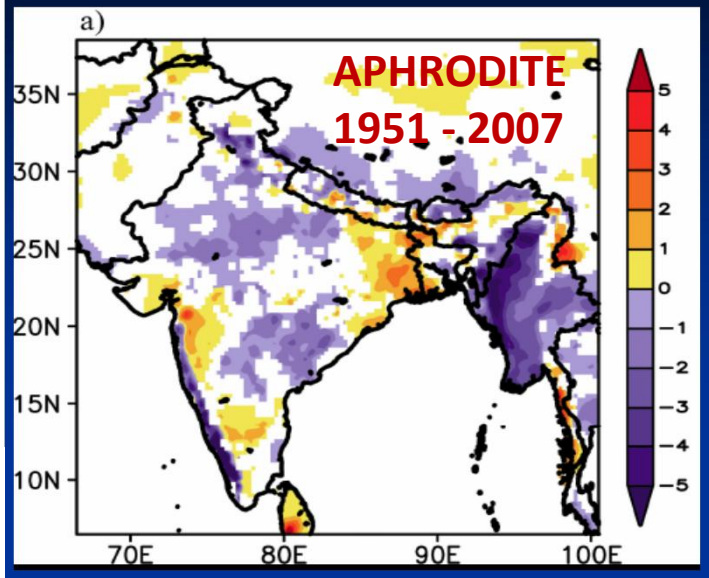

Increasing Trend of Extreme Rain Events over India in a Warming Environment

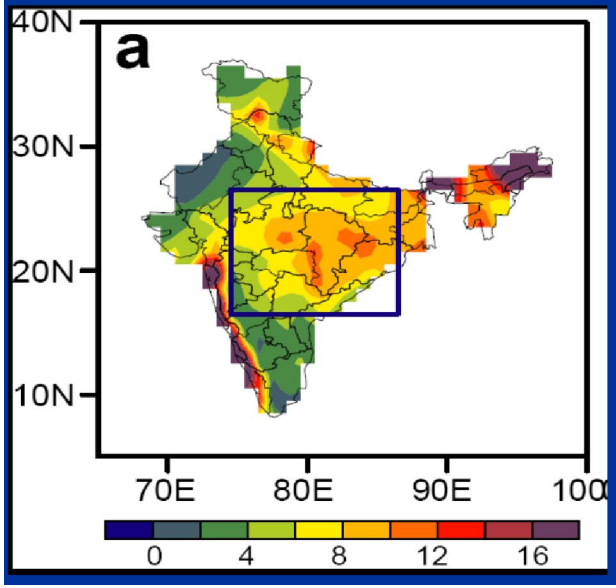

Goswami et al. 2006, Science

Time series of count over Central India

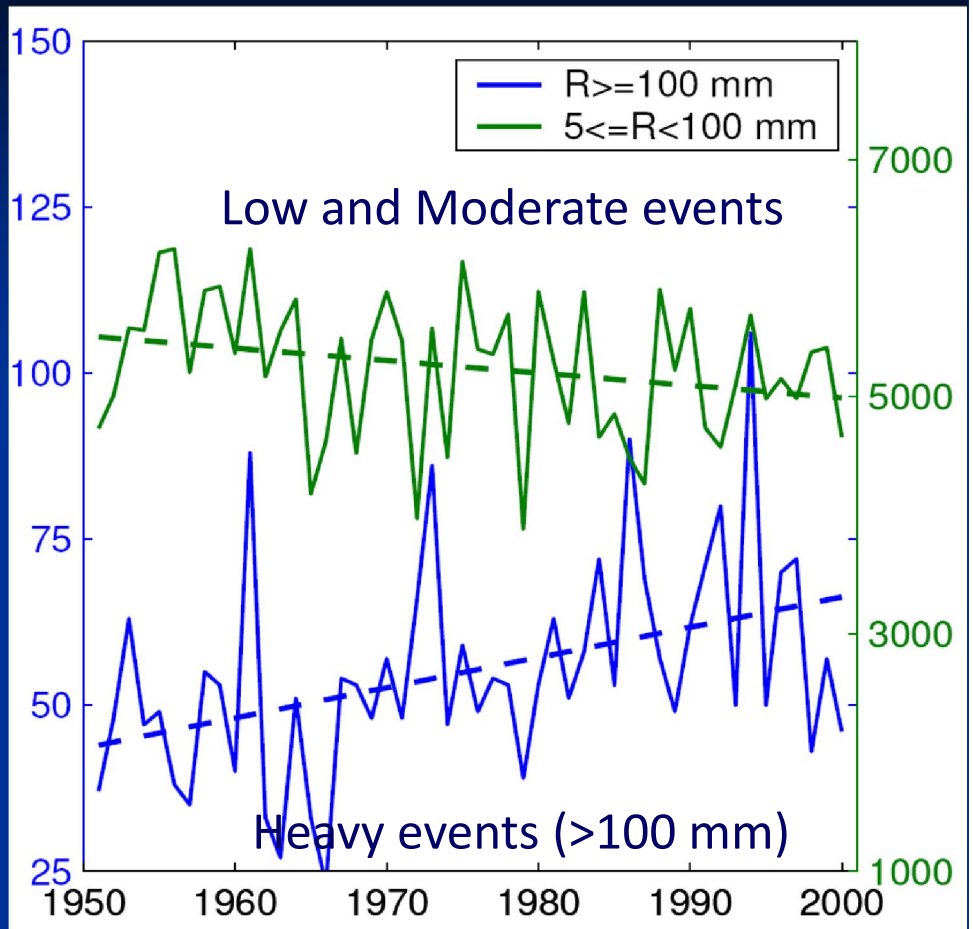

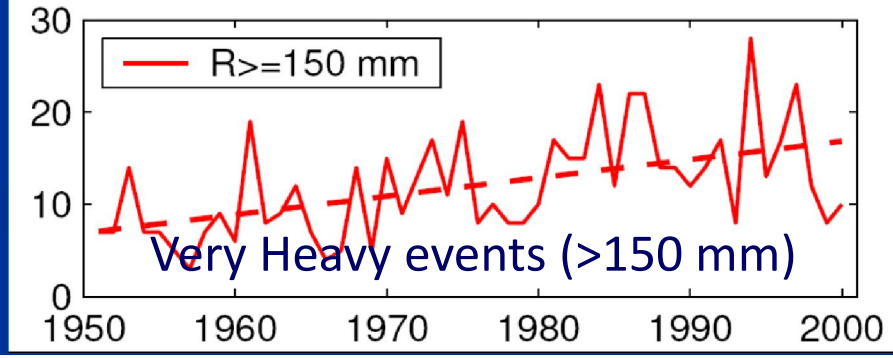

Interannual, Interdecadal and long-term trends of extreme rainfall events over Central India modulated by equatorial Indian Ocean SST variations –Rajeevan et al. 2008

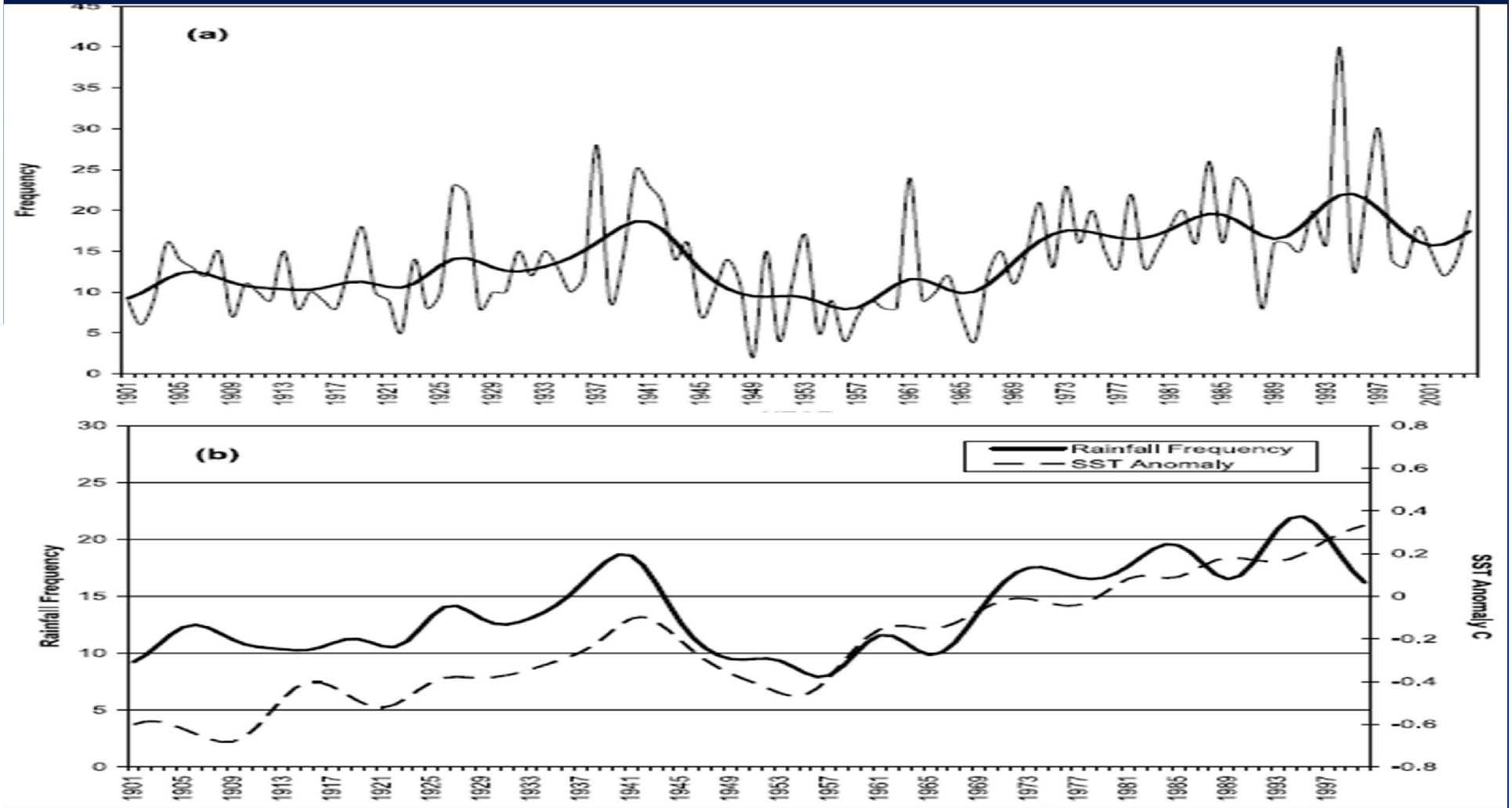

(a) Temporal variation of frequency of very heavy rainfall events (R > 150 mm/day) over Central India (thin line) and its smoothed variation (thick line) during 1901-2004 **(b)** Smoothed variation of frequency of very heavy rainfall events over central India and SST anomalies over Equatorial Indian ocean - Rajeevan et al. 2008 GRL

Anthropogenic forced changes in monsoon rainfall will remain difficult to detect against a backdrop of large natural variability – Sinha et al. Nature Comm. 2015

Reconstruction of Indian monsoon rainfall over the last two millenia using stable oxygen isotopes in speleothems from northern India over the last two millennia

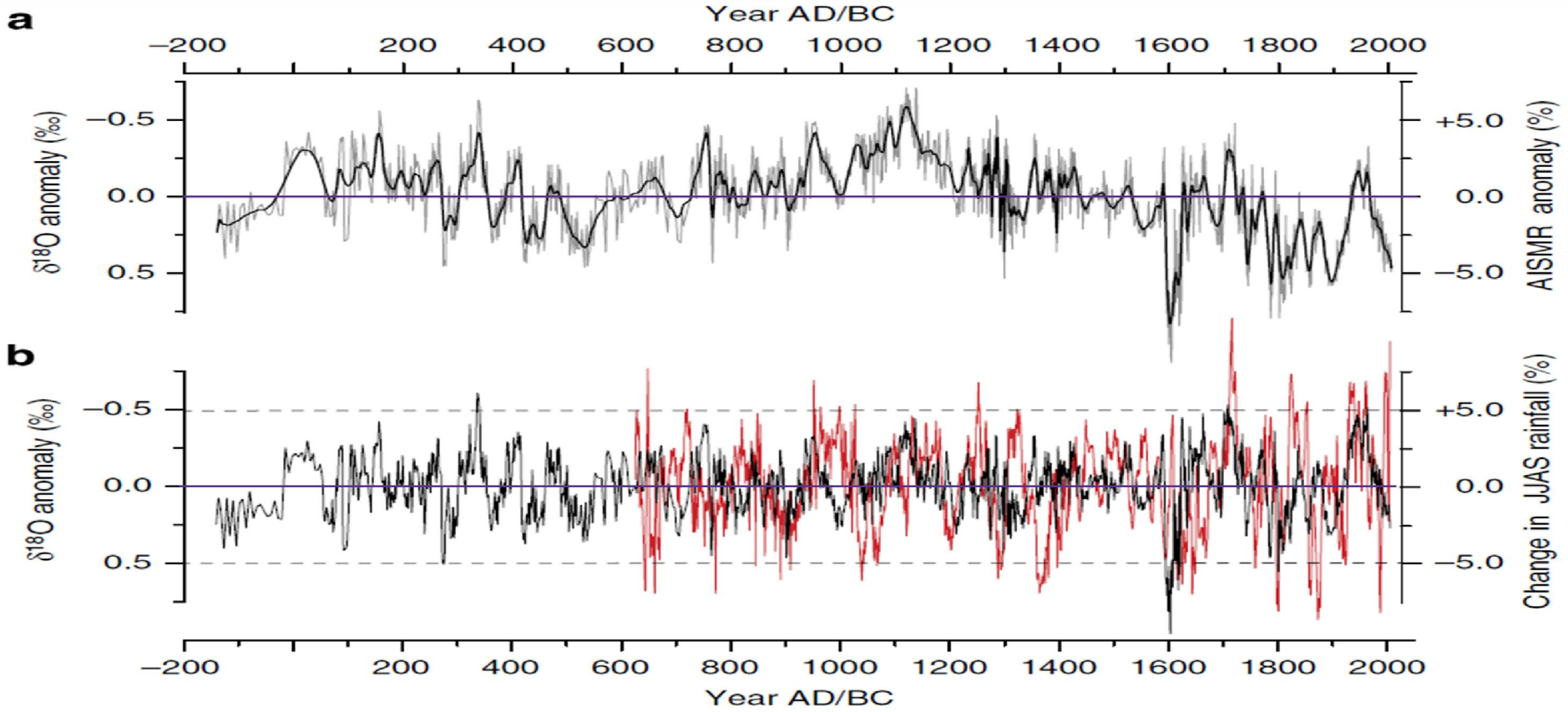

Figure 3 | Time series analysis of the NI and CI $\delta^{18}O$ records. (**a**) The NI speleothem record shown as $\delta^{18}O$ anomalies (relative to the mean of the time series). The $\delta^{18}O$ anomalies are shown both as raw data (grey) and smoothed (11-year running mean) (black) along with the regressed AISMR anomalies (%). (**b**) The comparison between the SSA[44] detrended NI (black) and CI[14–16] (red) speleothem records shown as $\delta^{18}O$ anomalies (raw data). The long-term non-stationary trends in both time series are removed by subtracting the first reconstructed component indicated by SSA of the raw data. The two dashed horizontal lines delineate a 10% change in monsoon rainfall amounts, highlighting the magnitude of multi-decadal variability inferred from our NI $\delta^{18}O$ record. (**c**) Power spectrum of the composite NI and (**d**) CI SSA-detrended $\delta^{18}O$ time series obtained using REDFIT[31] software. A varying number of Welch overlaps were used to optimize bias/variance properties. Spectral band significant above the 90% level are labelled with their period.

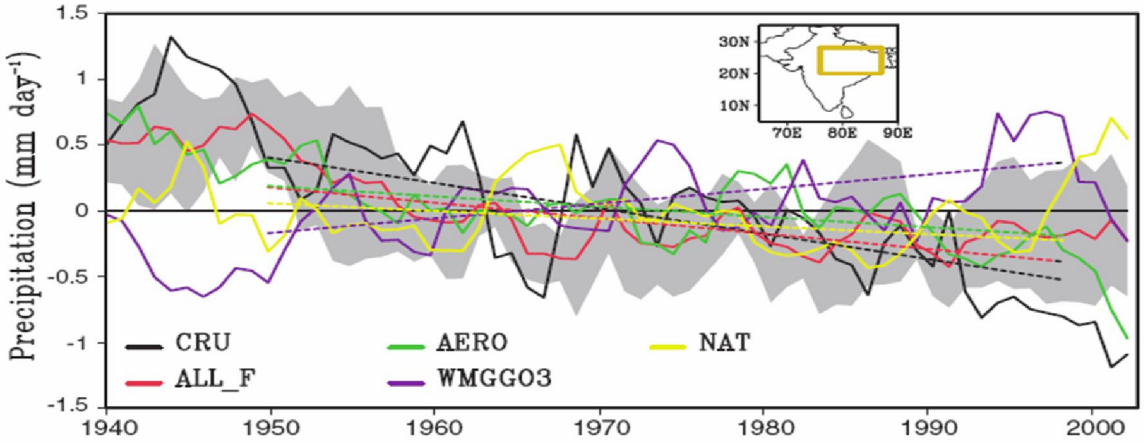

Anthropogenic Aerosols and the Weakening of the South Asian Summer Monsoon

Massimo A. Bollasina *et al.*

Science **334**, 502 (2011);

DOI: 10.1126/science.1204994

Bollasina, Ming and Ramaswamy
Science, 2011

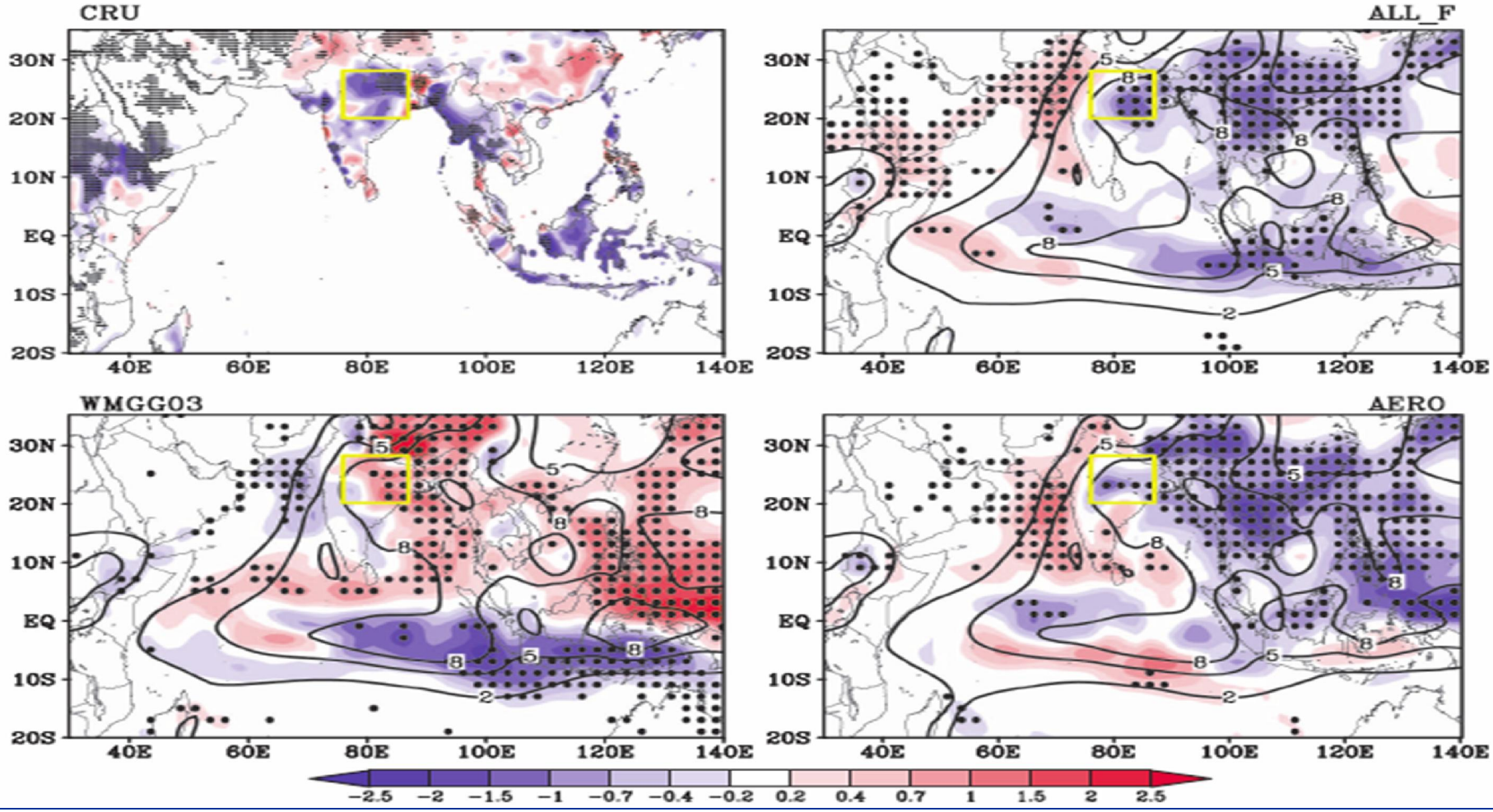

Deciphering the desiccation trend of the South Asian monsoon hydroclimate in a warming world

R. Krishnan[1] · T. P. Sabin[1] · R. Vellore[1] · M. Mujumdar[1] · J. Sanjay[1] · B. N. Goswami[1,2] · F. Hourdin[3] · J.-L. Dufresne[3] · P. Terray[4,5]

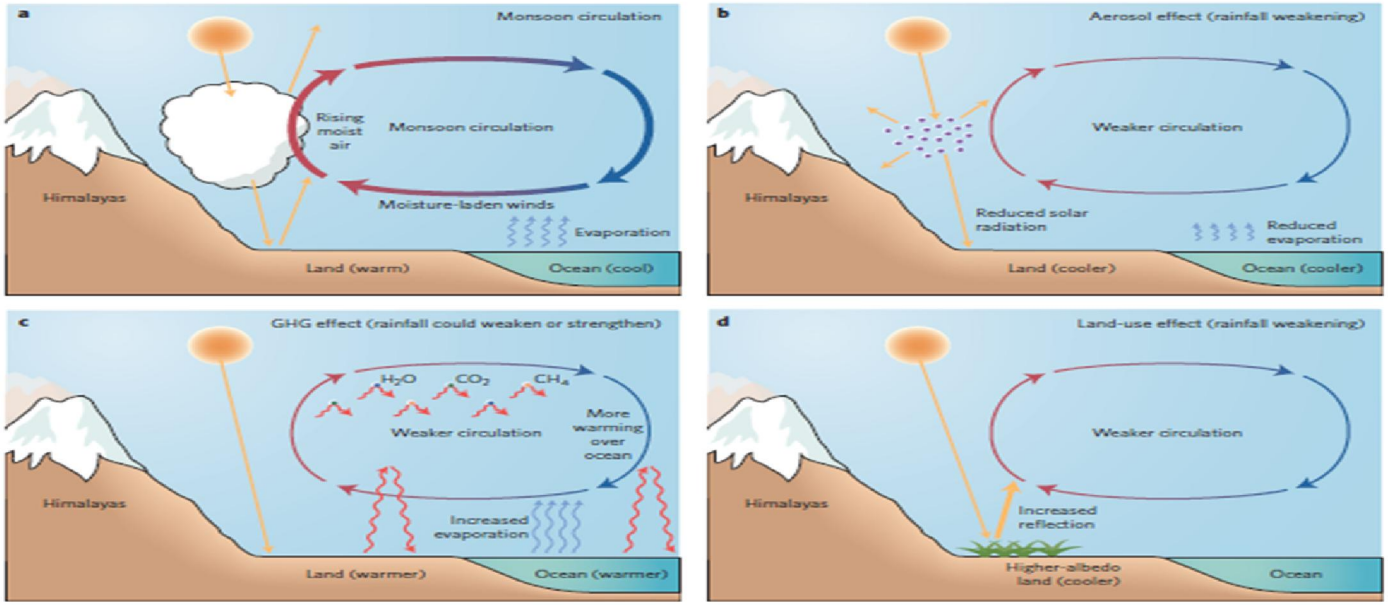

The onset of the monsoon in early June brings with it a burst of life across the region — children playing on the streets, blossoming flora, flowing rivers, and sowing of agricultural lands. The monsoon supplies ~80% of South Asia's annual rainfall, supporting the region's primarily rain-fed agriculture and recharging rivers, aquifers and reservoirs that provide water to over one-fifth of the global population. Since the 1950s, the monsoon has weakened[1] and become more erratic, with increased occurrence of extreme rainfall events[2]. This has led to crop failures and water shortages with severe socio-economic and humanitarian impacts across South Asia. Writing in *Climate Dynamics*, R. Krishnan and colleagues[3] suggest that anthropogenic greenhouse gas (GHG) emissions, aerosol emissions and agricultural land-cover changes are responsible for the observed changes in rainfall patterns. They predict that the monsoon weakening will continue through the twenty-first century, threatening the livelihoods and resources of over 1.6 billion people in the region.

SOUTH ASIAN MONSOON

Tug of war on rainfall changes

Rainfall associated with the South Asian summer monsoon has decreased by approximately 7% since 1950, but the reasons for this are unclear. Now research suggests that changes in land-cover patterns and increased emissions from human activities have contributed to this weakening, which is expected to continue in the coming decades.

LMDZ grid setup for CORDEX South Asia (shaded region has grid-size < 35 km)

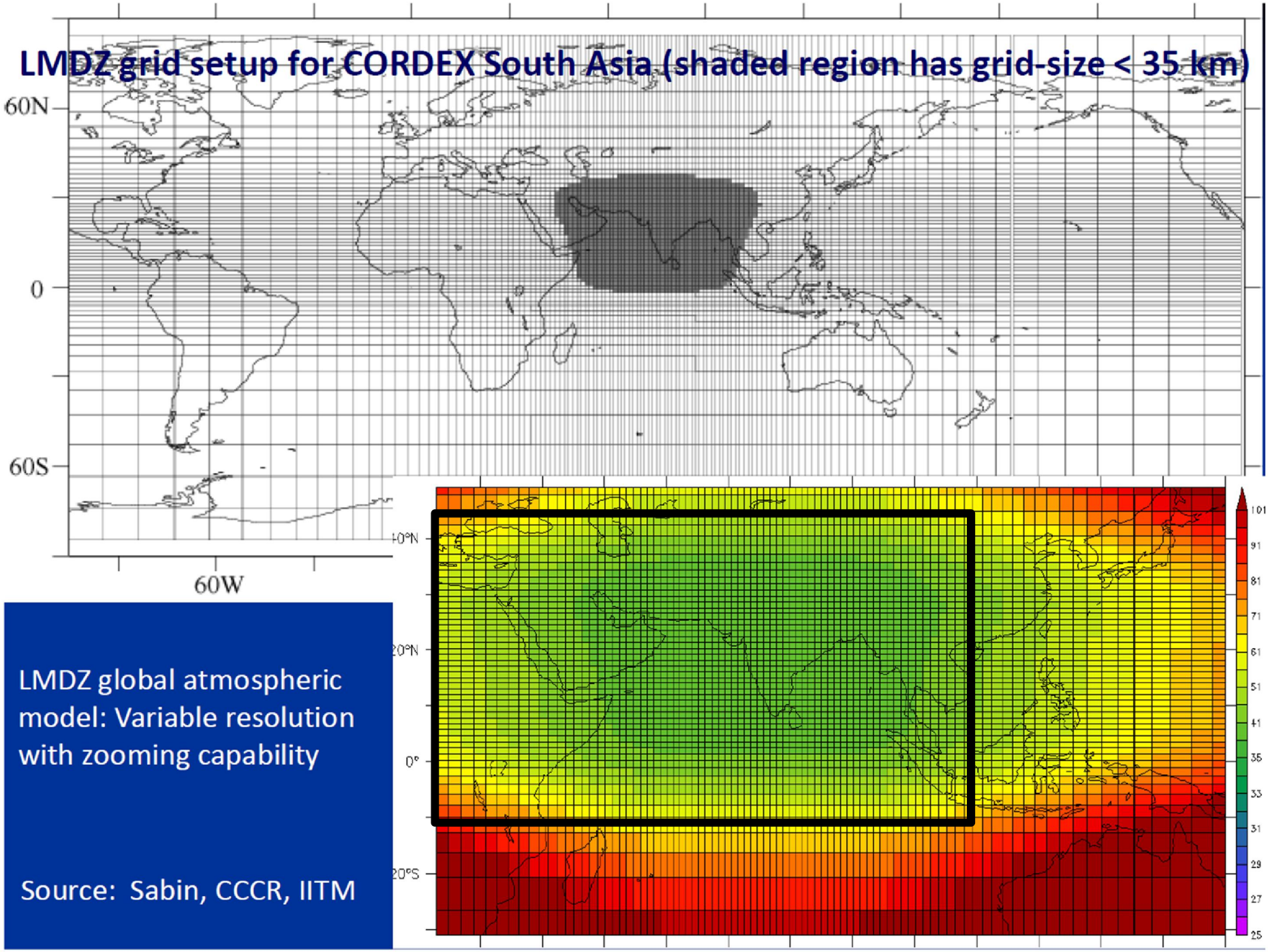

LMDZ global atmospheric model: Variable resolution with zooming capability

Source: Sabin, CCCR, IITM

Global climate

No zoom: 1°x1° ; **Zoom**: same number of points, with resolution ≈35 km over west Asia

precip JJAS (mm/day)

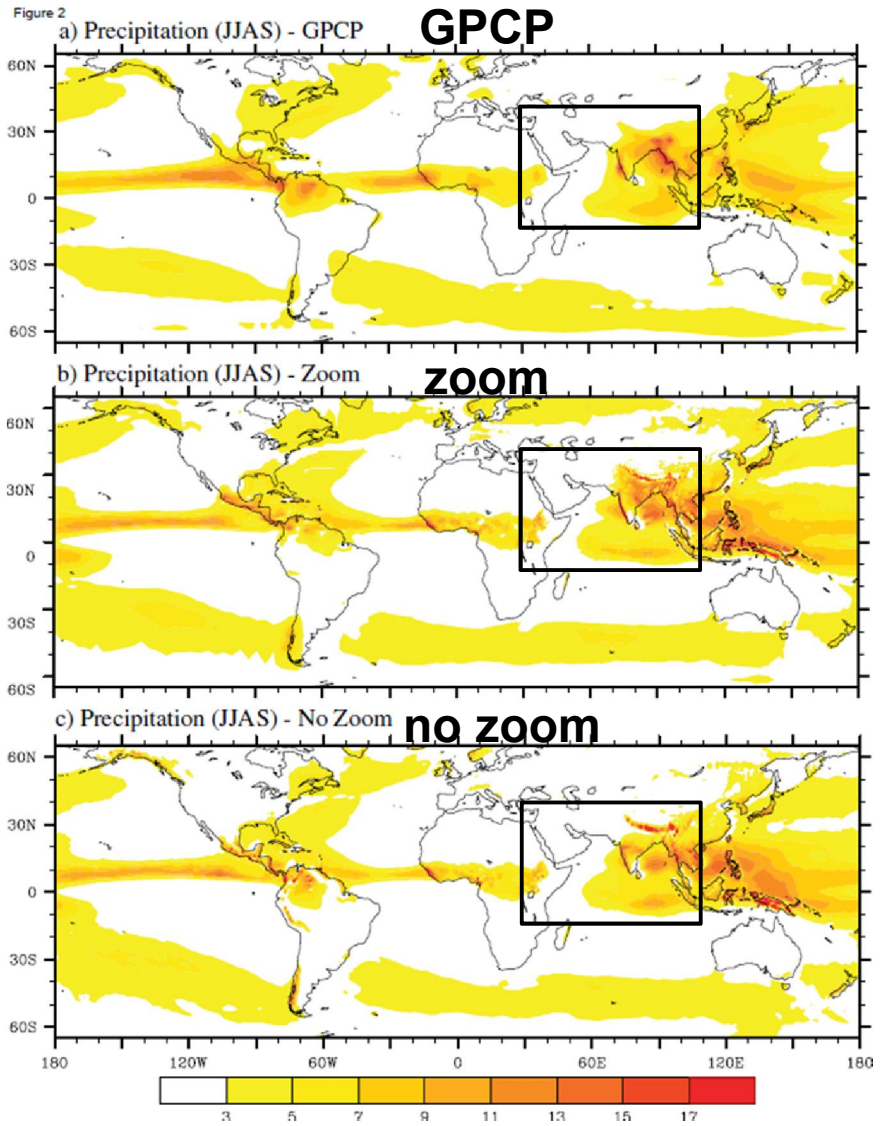

Mean winds at 850 hPa (JJAS)

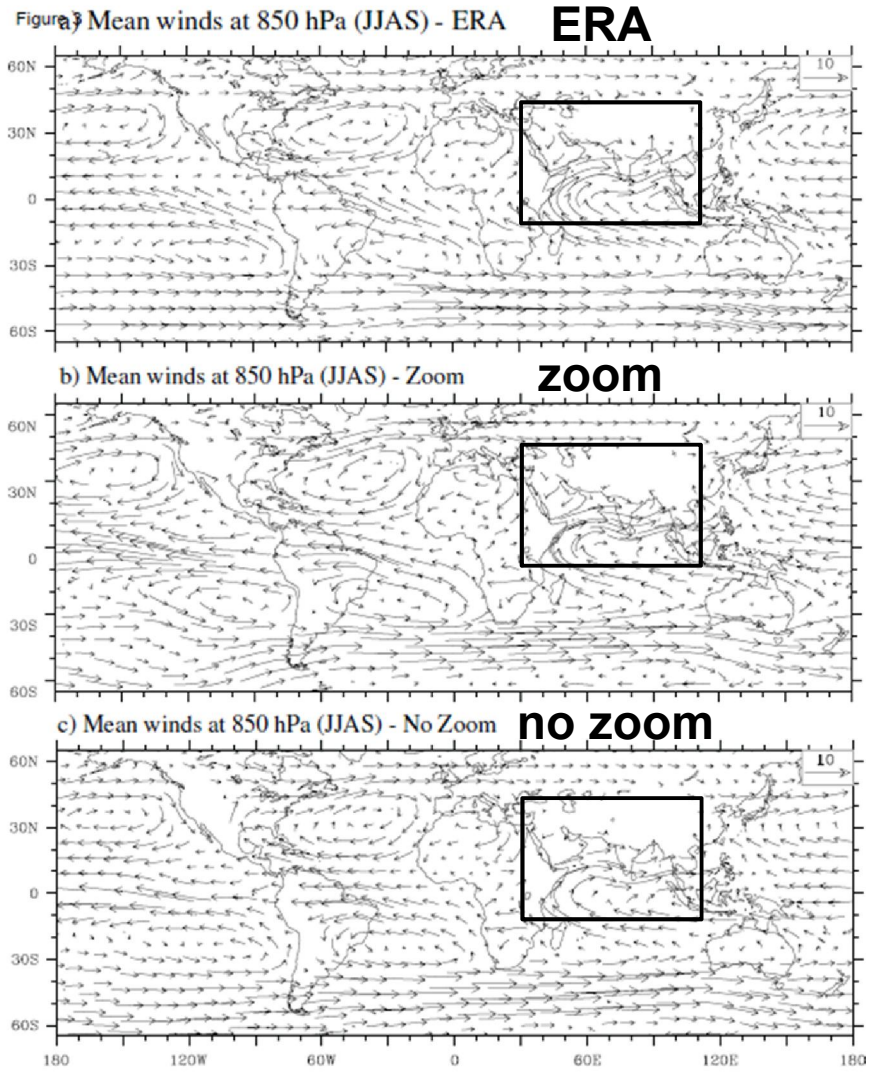

South Asia CORDEX domain

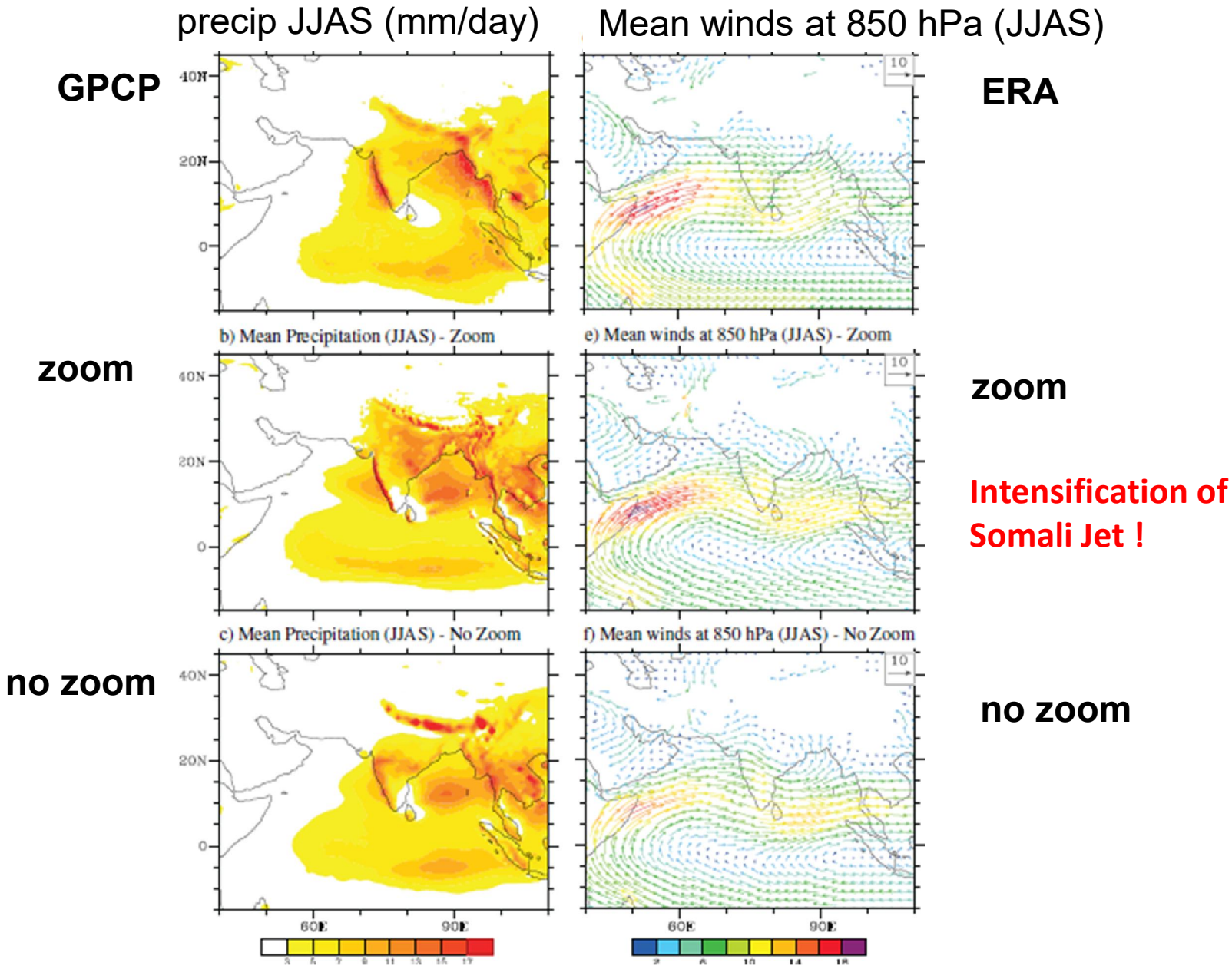

Climatological results

Rainfall and surface temperature over the Indian landmass

JJAS mean rainfall

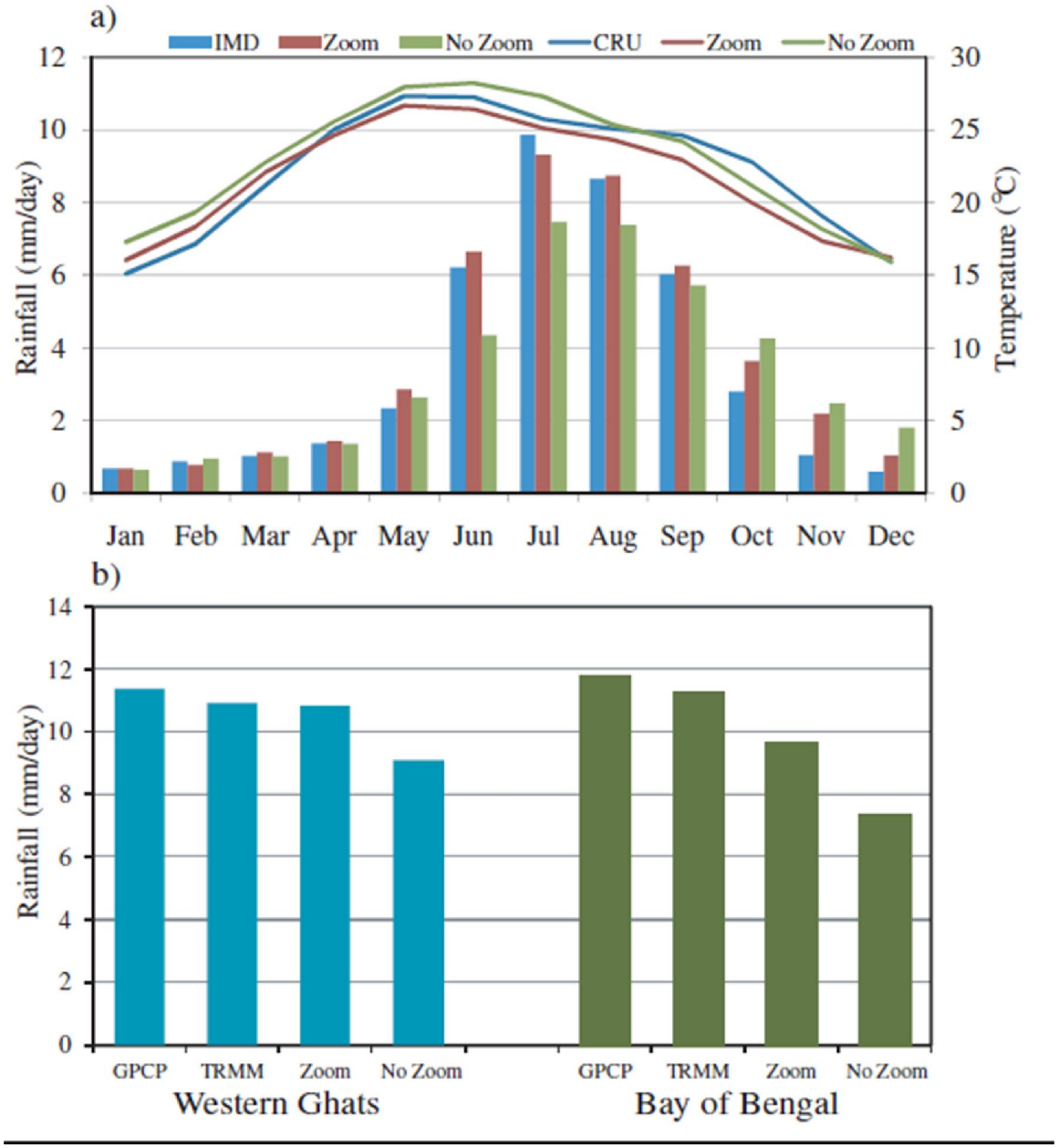

Total precipitable water (JJAS)

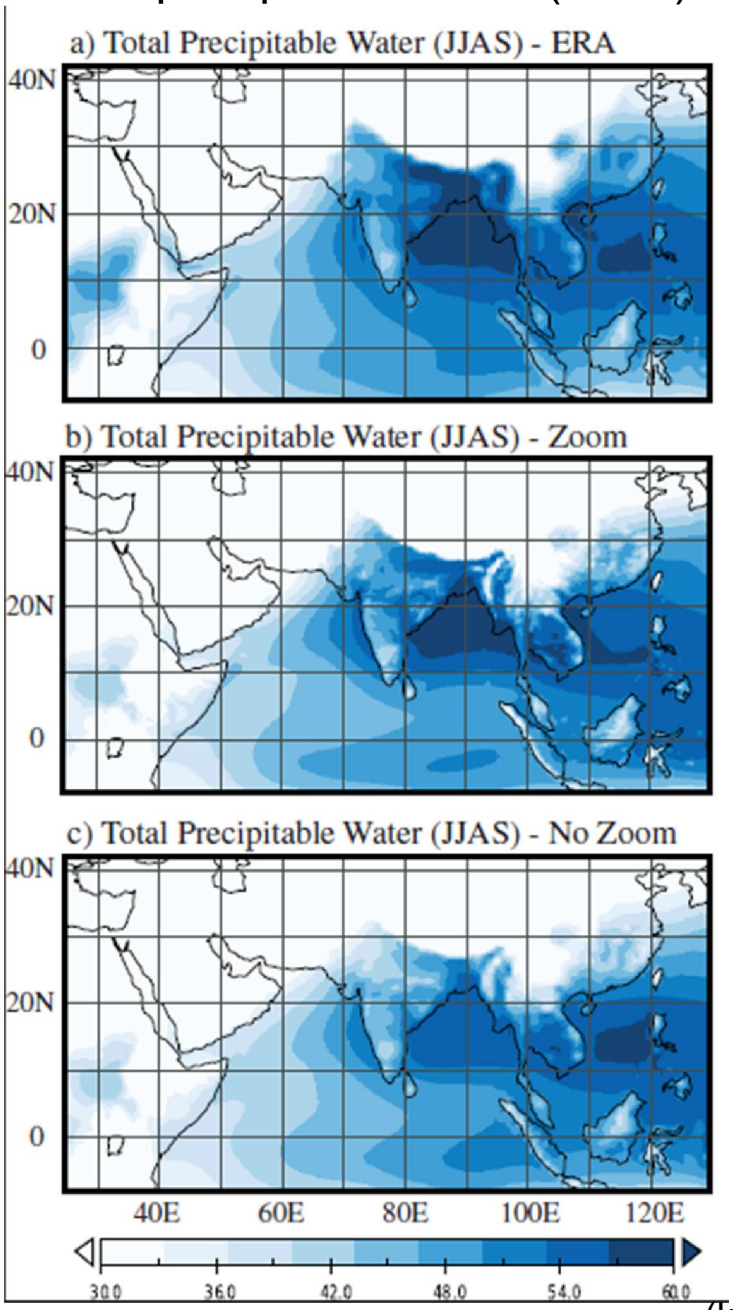

(kg.m^{-2})

Specific humidity (JJAS)

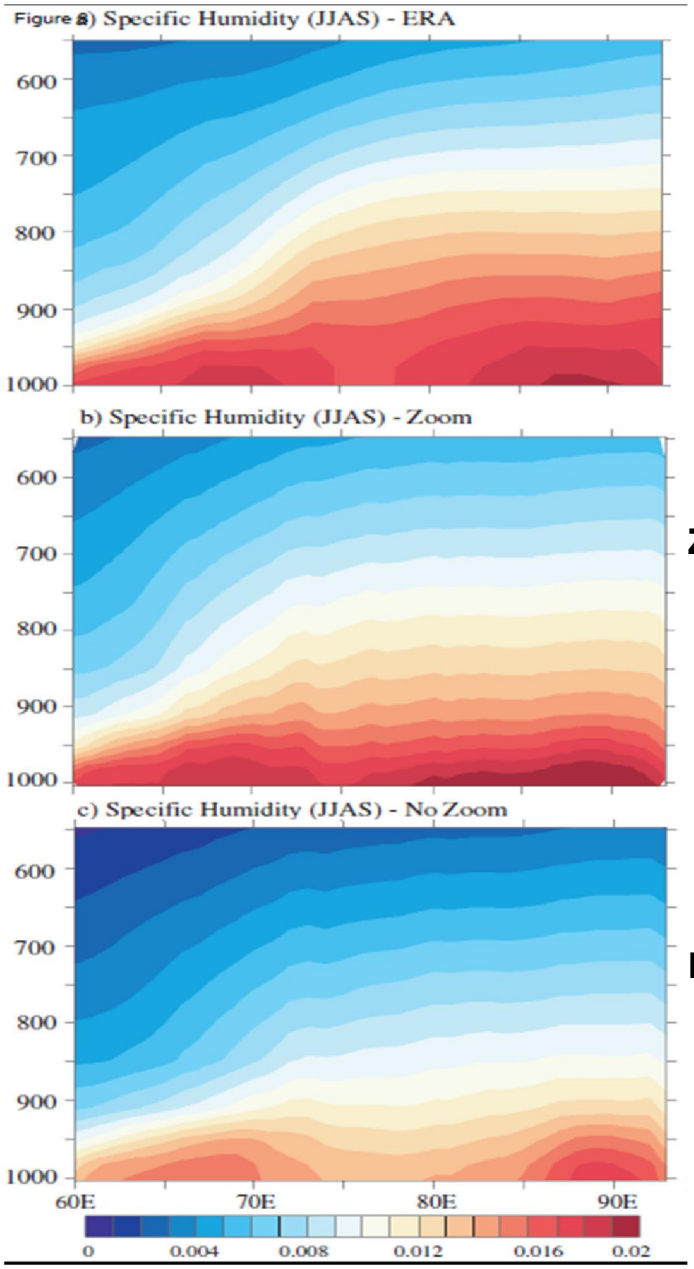

ERA

zoom

no zoom

(kg.kg^{-1})

Moist Static Energy (x 10^3 Jm^{-2})

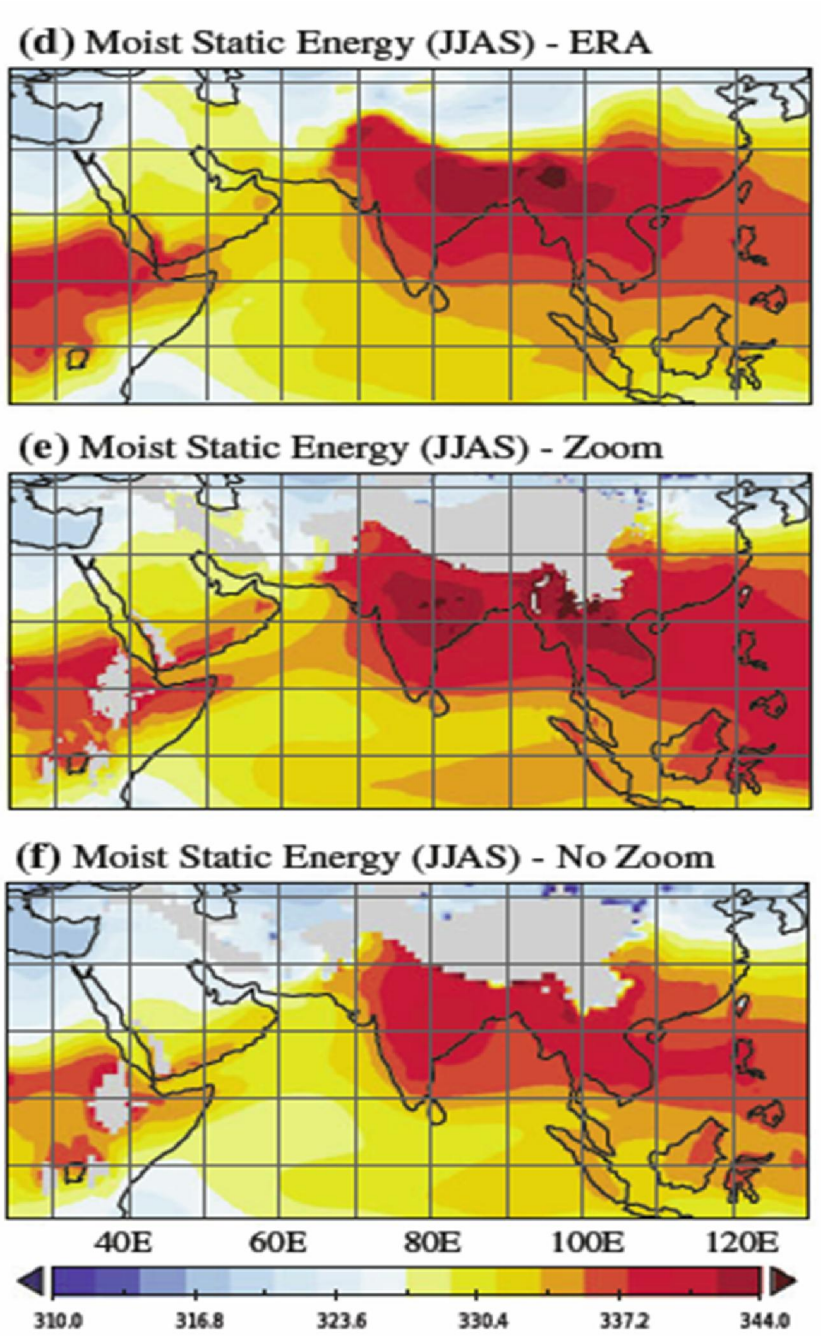

Vertical profiles [16N-28N, 65E 100E]

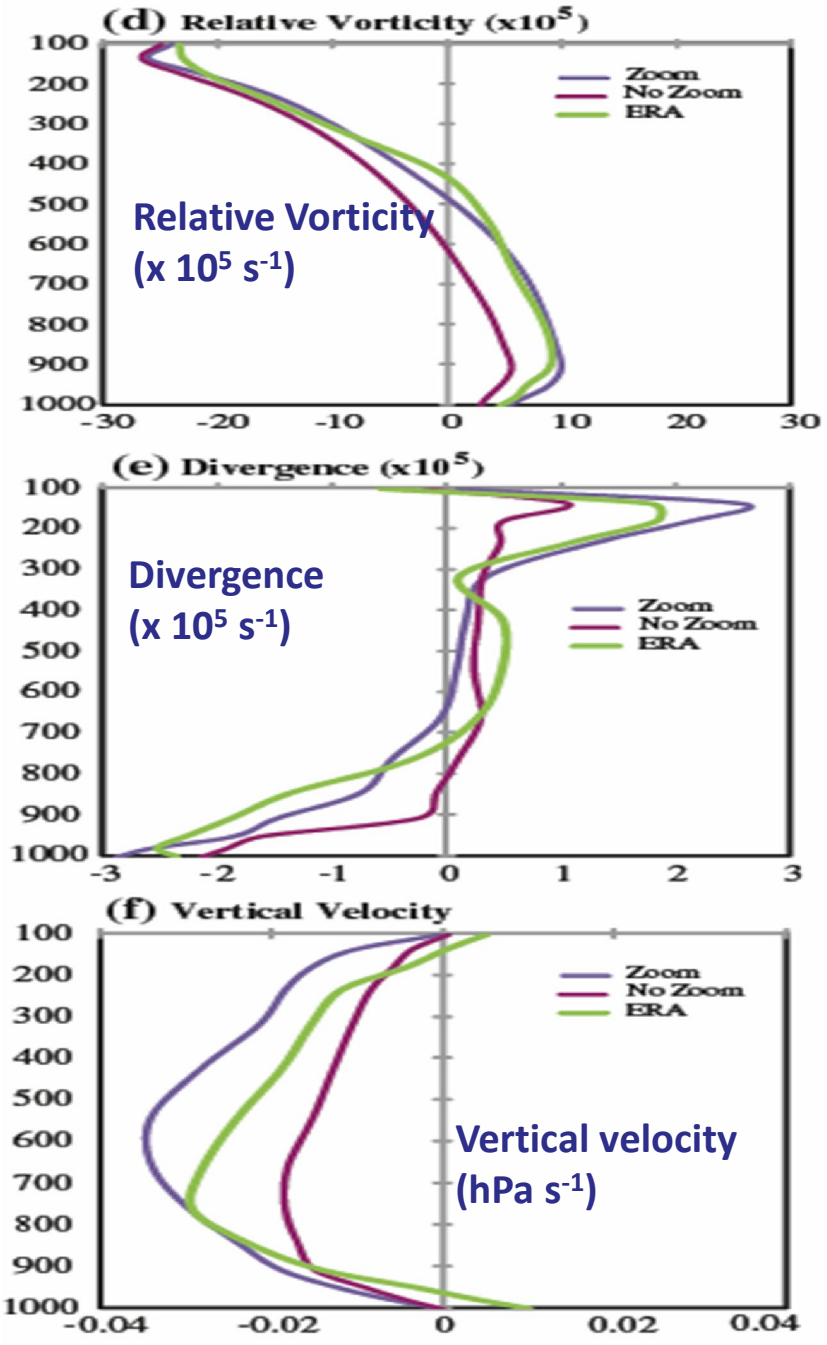

Patterns generated by regressing the 850 hPa winds on the index of frequency count (FC) of moderate-to-heavy rainfall.
Shading: magnitude of the regression. Unit of regression is ms^{-1} $(std.dev\ FC)^{-1}$.

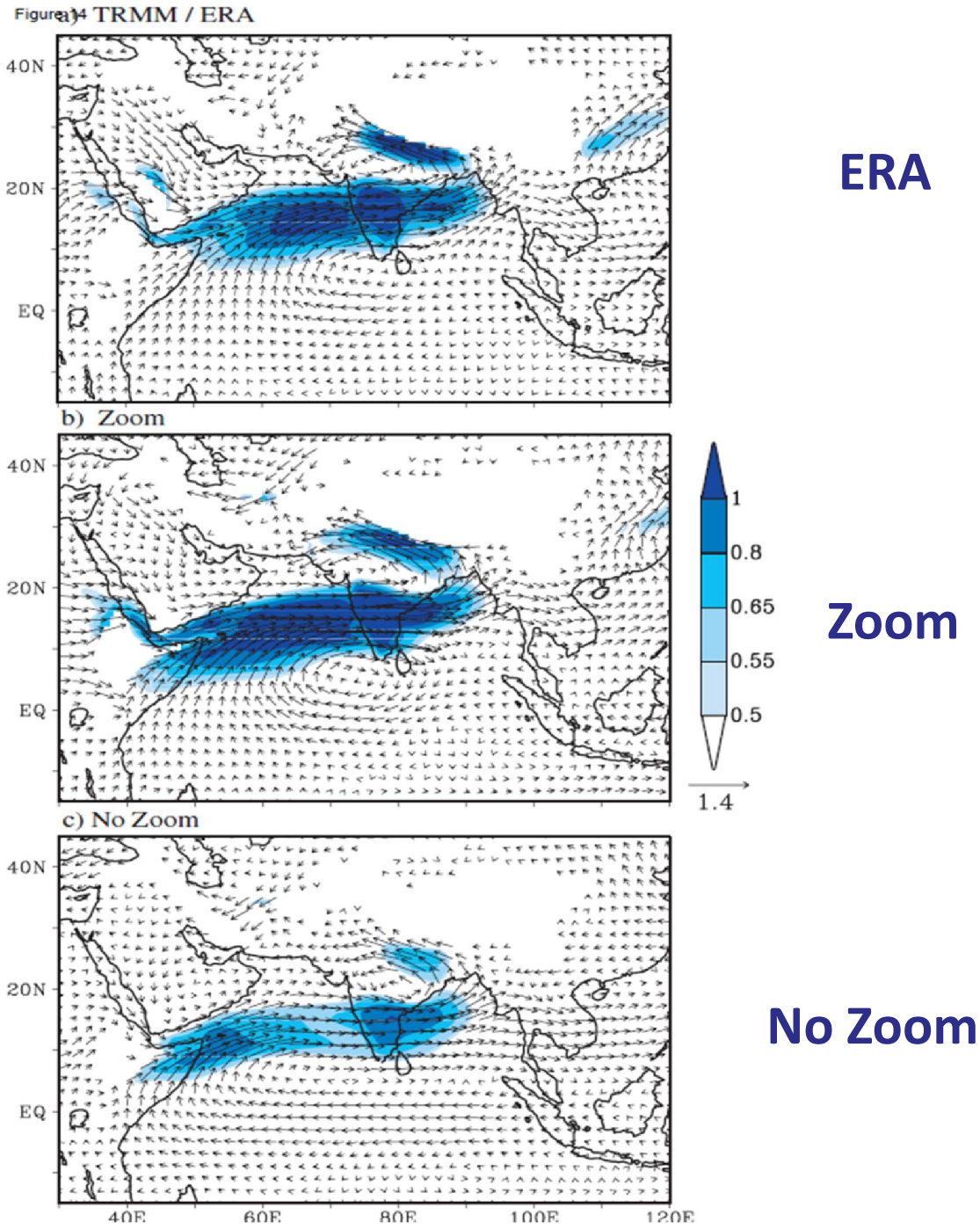

ERA

Zoom

No Zoom

JJAS mean (1951-2005): Source: Ramarao et al. (2015) Earth Sys. Dynam

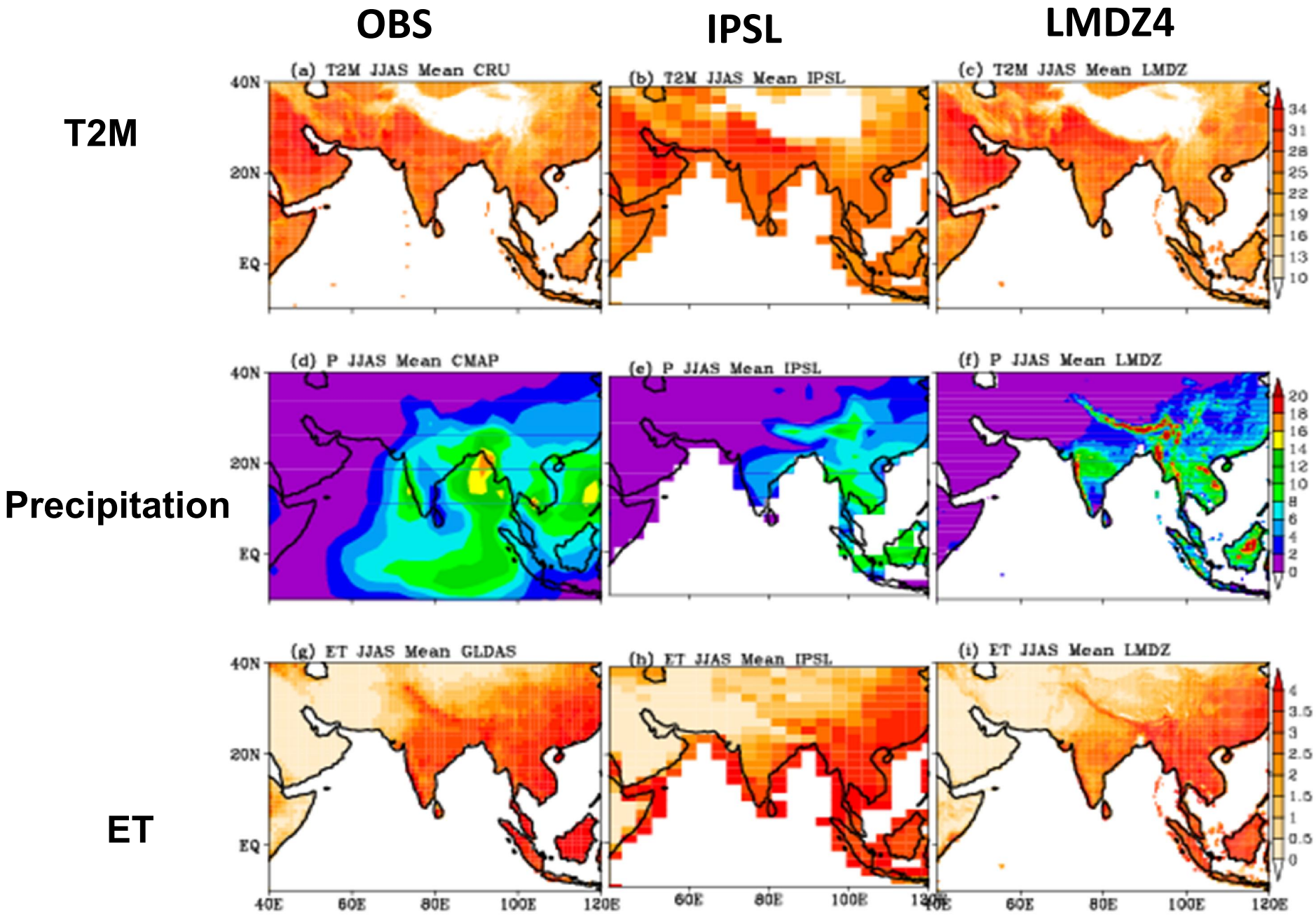

Annual mean water balance (mm d^{-1}) components: (1979-2005)

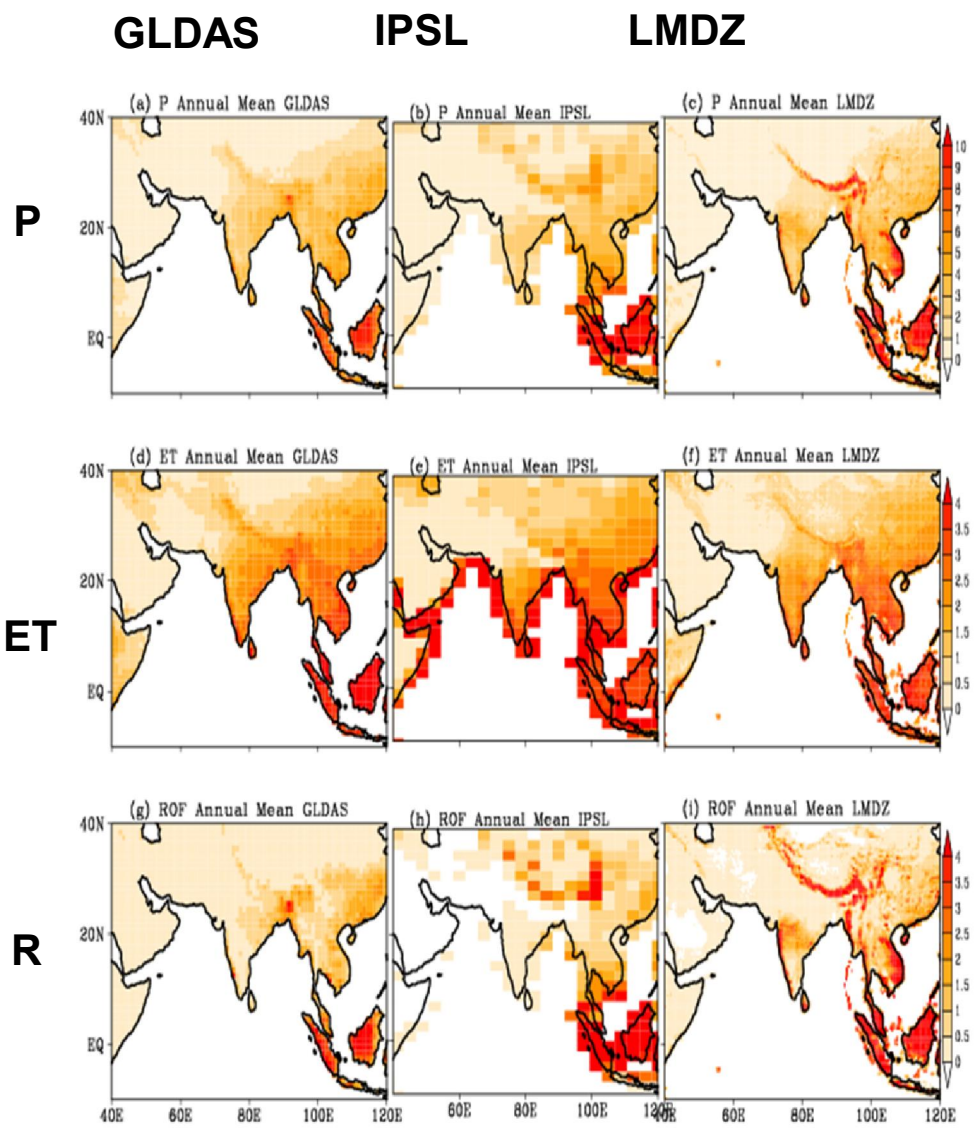

Water balance averaged over
70°-90°E;10°-28°N

	GLDAS	IPSL	LMDZ
P	2.63	1.81	2.97
ET	1.99	2.25	1.92
R	**0.65**	**0.28**	**1.06**
P-ET	**0.64**	**-0.44**	**1.05**

The water balance is highlighted

Source: MVS. Ramarao, R. Krishnan
J. Sanjay, TP. Sabin (2015): ESD

Recent Climate change: IPCC 2013 report

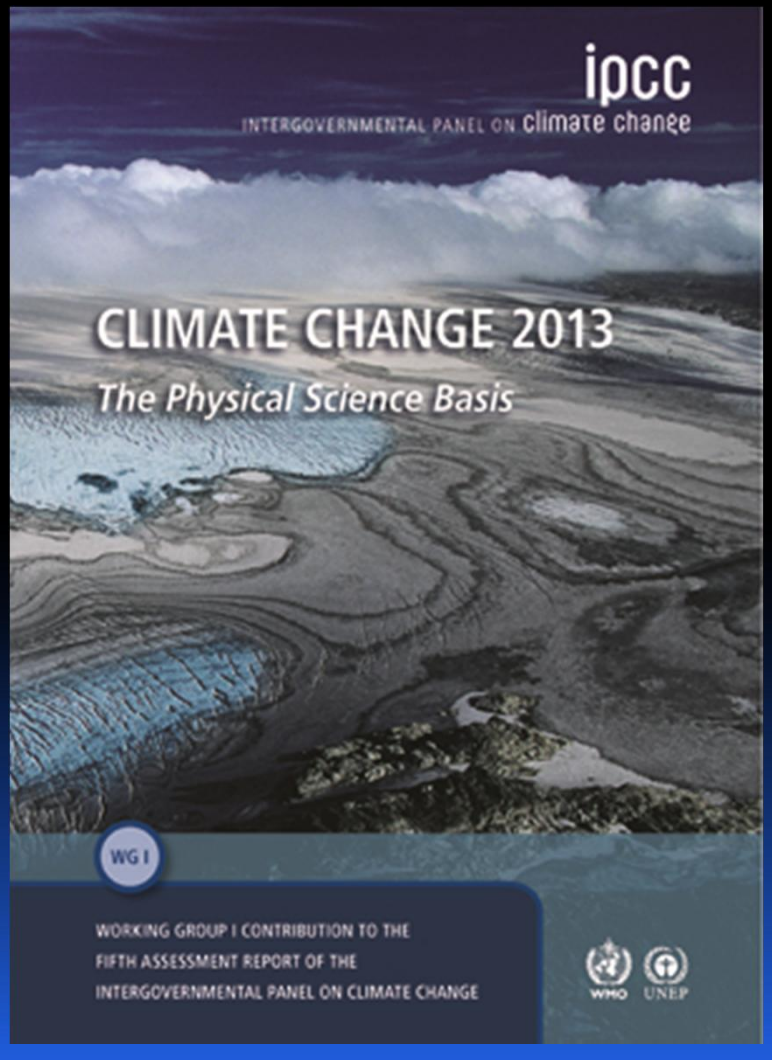

Warming of the climate system is unequivocal, and since the 1950s, many of the observed changes are unprecedented over decades to millennia.

Recent climate change report

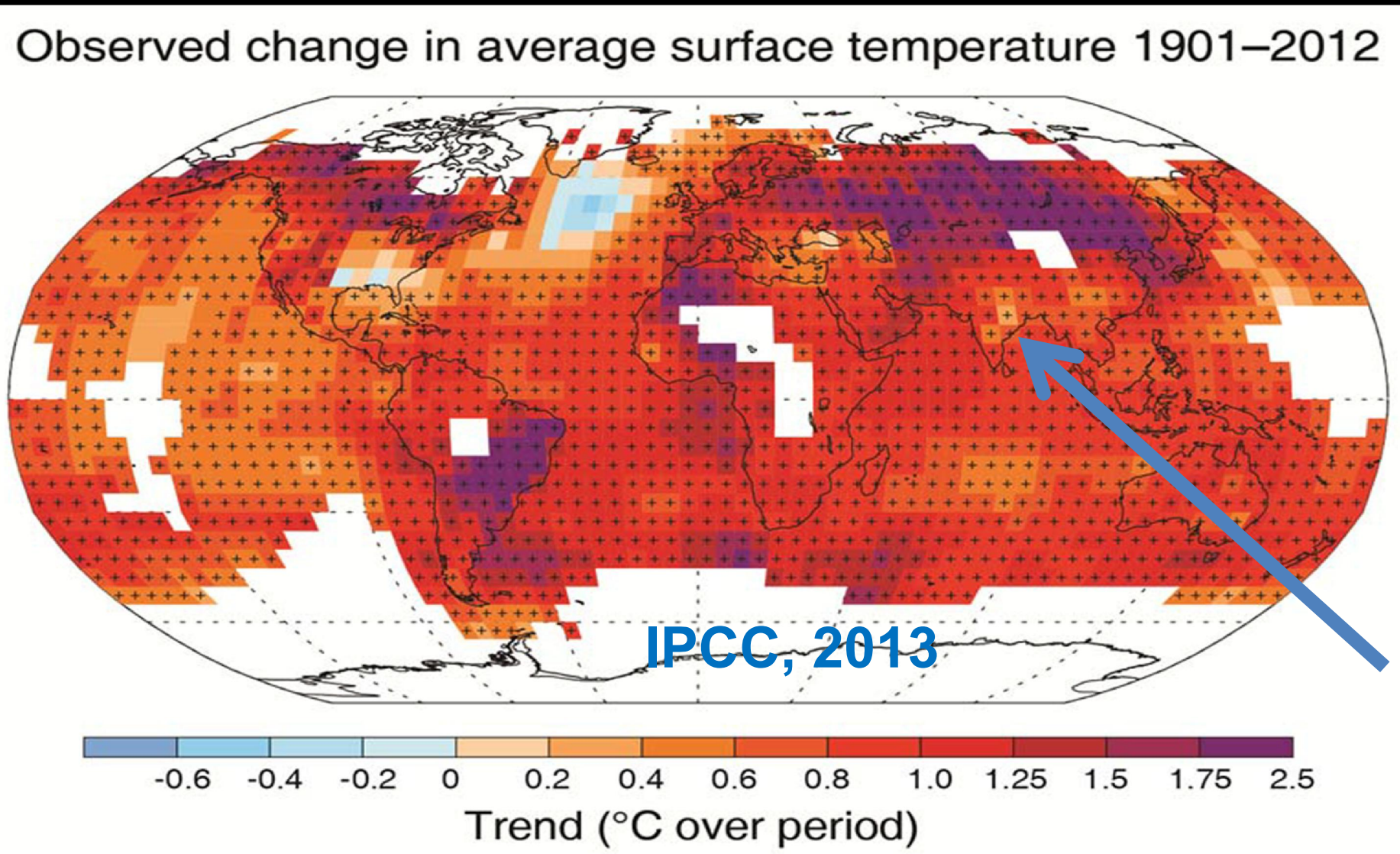

Planet has warmed by 0.85 K over 1880-2012

The Water Vapor Feedback

Temp dependence of saturation vapor pressure

$$e_s: e^{-5400/T}$$

$$\frac{d \ln e_s}{dT} = \frac{5400}{T^2} \approx 0.06 \quad to \quad 0.1 \quad per \quad K$$

Projected rainfall Change (2081-2100)

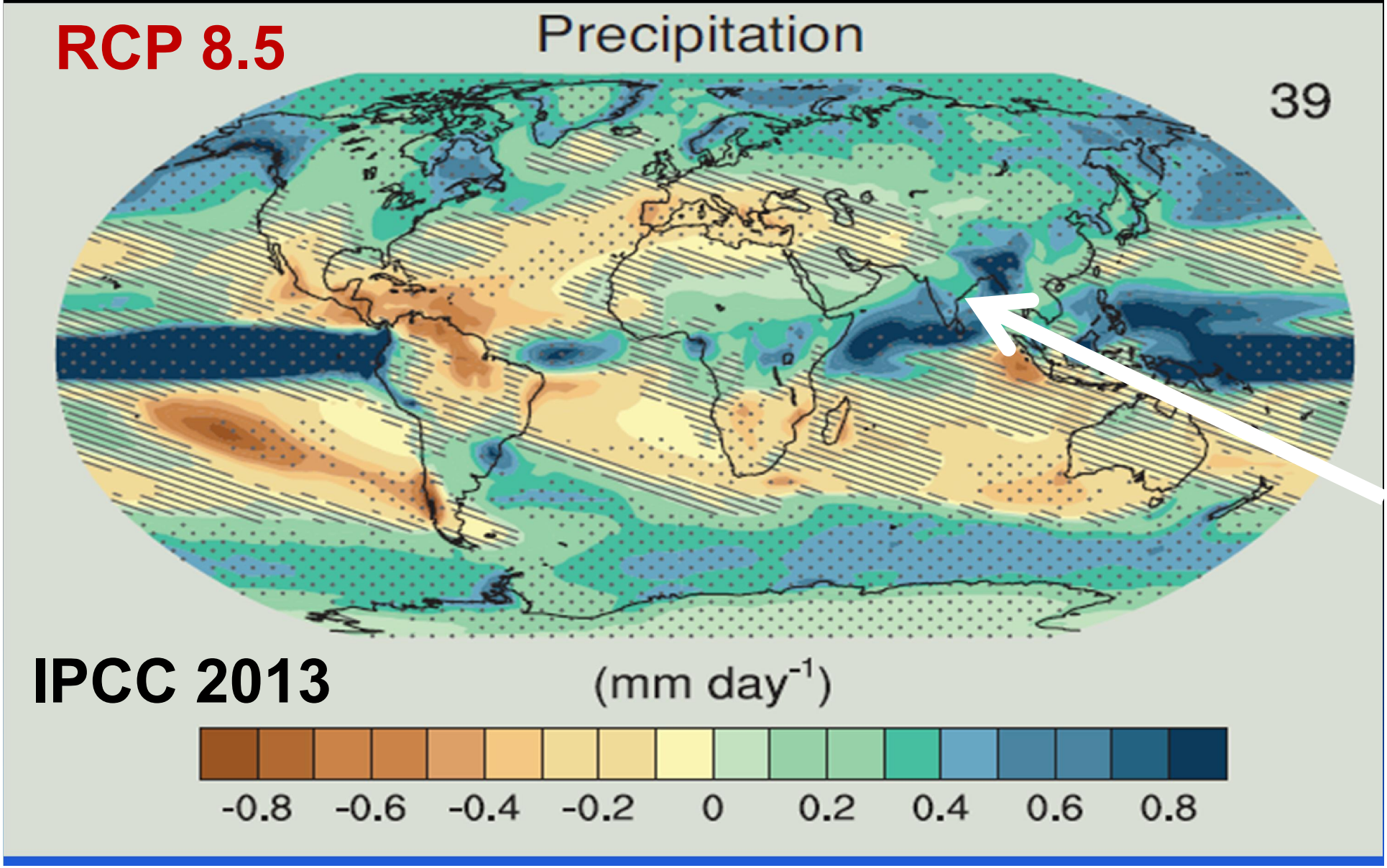

Wide variations among CMIP5/ CMIP3 models in capturing the South Asian monsoon

Indian Land: CMIP5 vs Obs

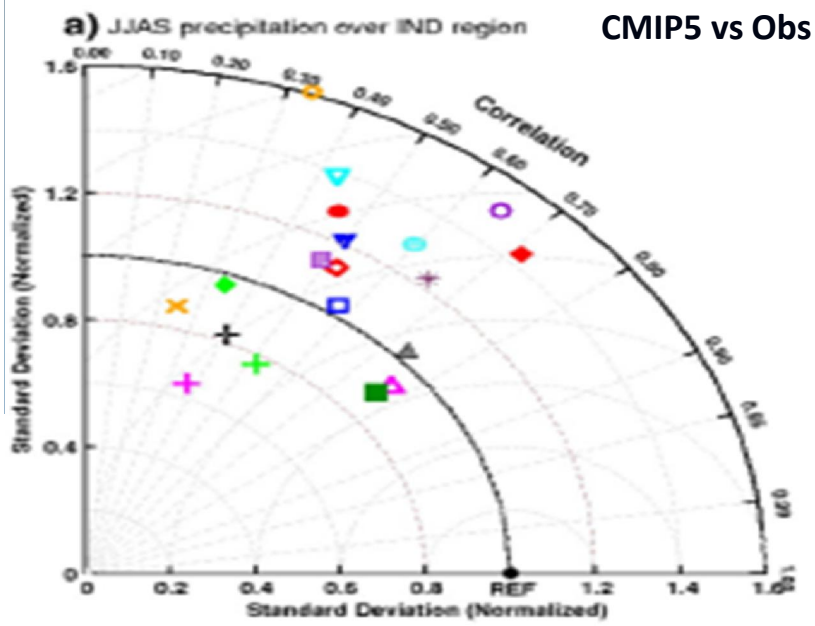

ISM domain 15S-30N, 50E-120E

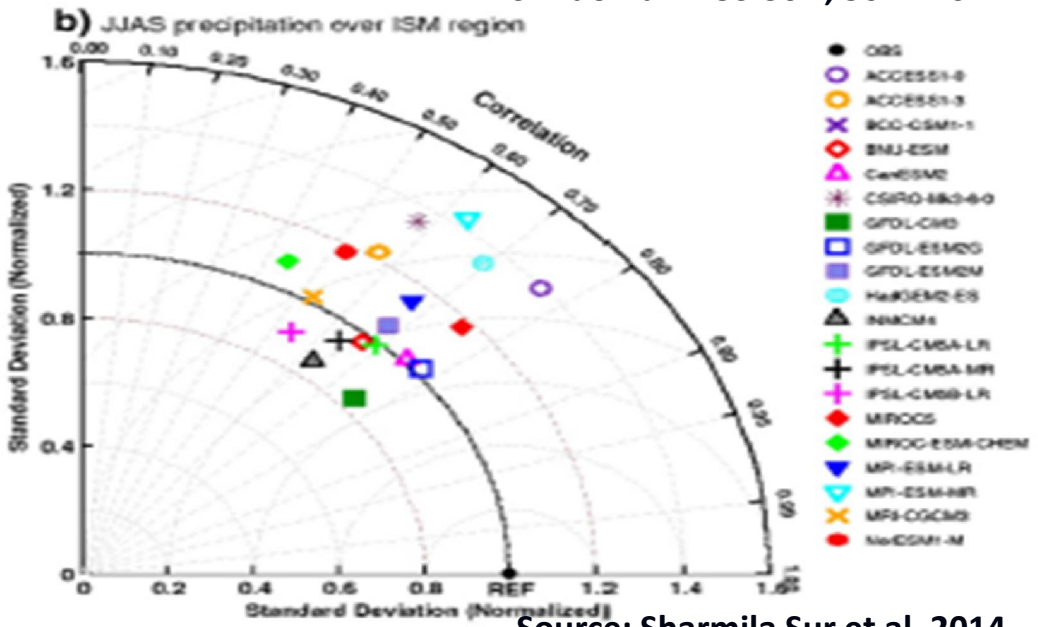

Source: Sharmila Sur et al. 2014

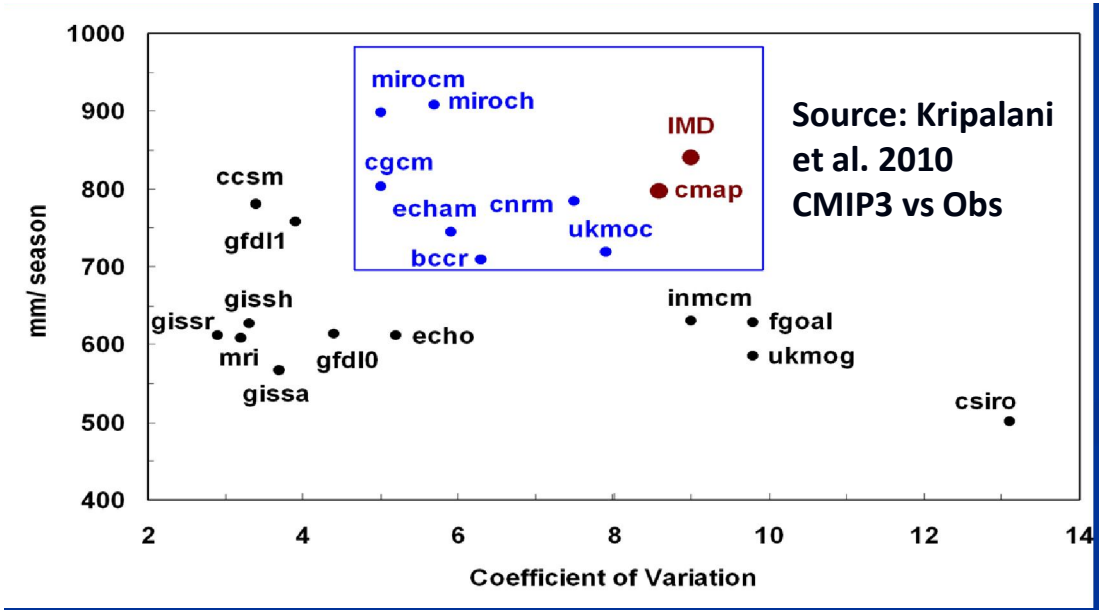

Source: Kripalani et al. 2010
CMIP3 vs Obs

Realism of present-day climate simulation is an essential requirement for reliable assessment of future changes in monsoon

South Asian Climate Change

Source: IPCC, 2013 (Annex 1)

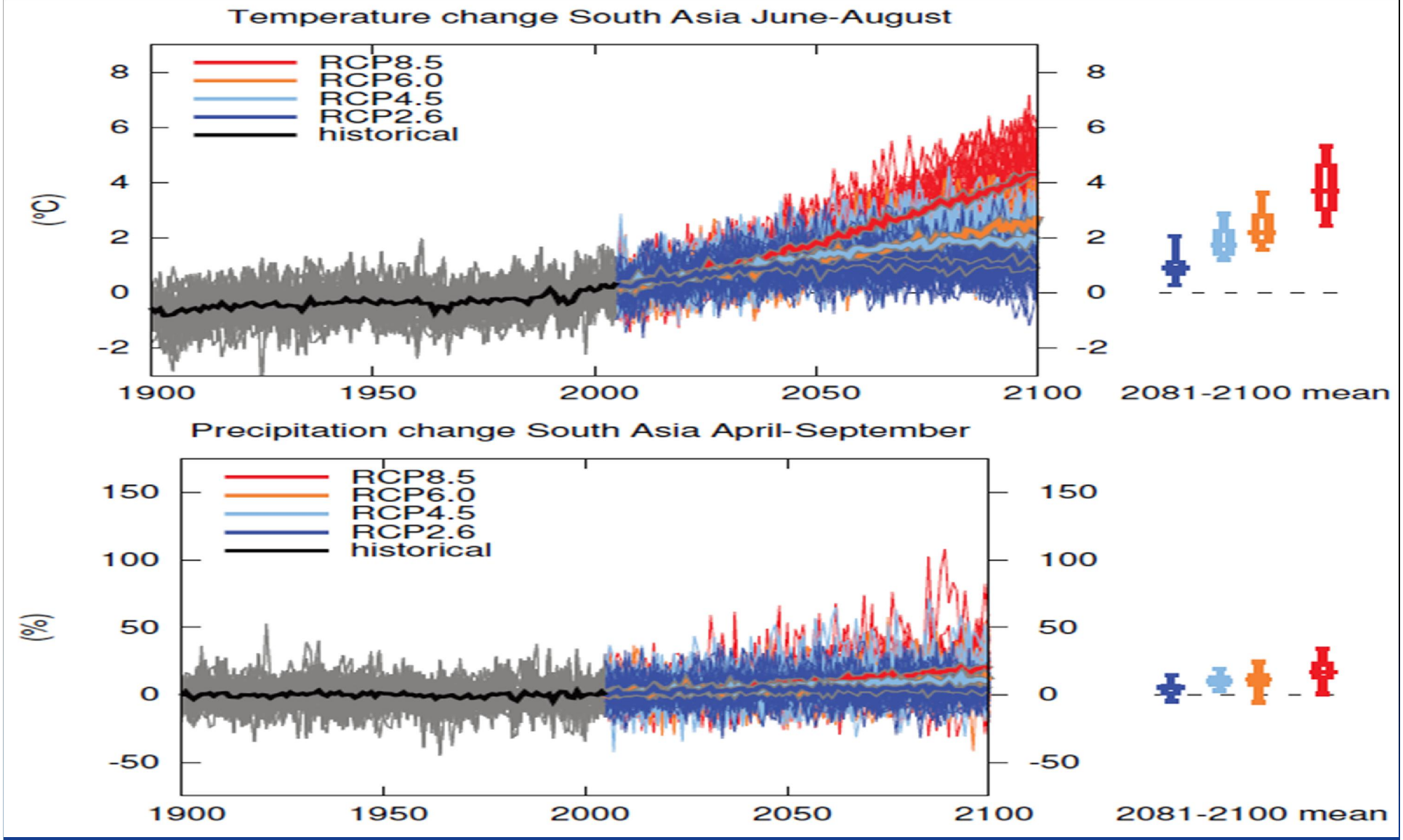

For high emission scenario, ensemble mean warming is about 4 K and precipitation change is about 15%

High-resolution (~ 35 km) modeling of **climate change over S.Asia**

Historical (1886-2005):

Includes natural and anthropogenic (GHG, aerosols, land cover etc) climate forcing during the historical period (1886 – 2005) ~ 120 years

Historical Natural (1886 – 2005):

Includes only natural climate forcing during the historical period (1886– 2005) ~ 120 yrs

RCP 4.5 scenario (2006-2100) ~ 95 years:

Future projection run which includes both natural and anthropogenic forcing based on the IPCC AR5 RCP4.5 climate scenario. The evolution of GHG and anthropogenic aerosols in RCP4.5 produces a global radiative forcing of + 4.5 W m^{-2} by 2100

Runs performed on PRITHVI, CCCR-IITM

CO2 concentration in future IPCC AR5 scenarios

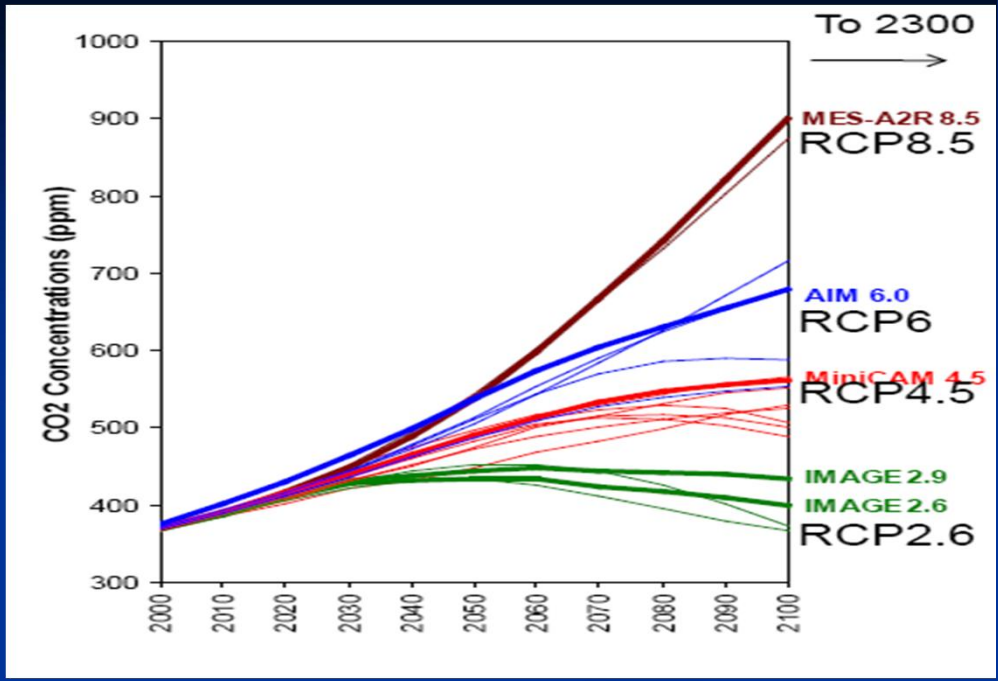

Aerosol distribution from IPSL ESM

INCA: INteraction with Chemistry and Aerosol

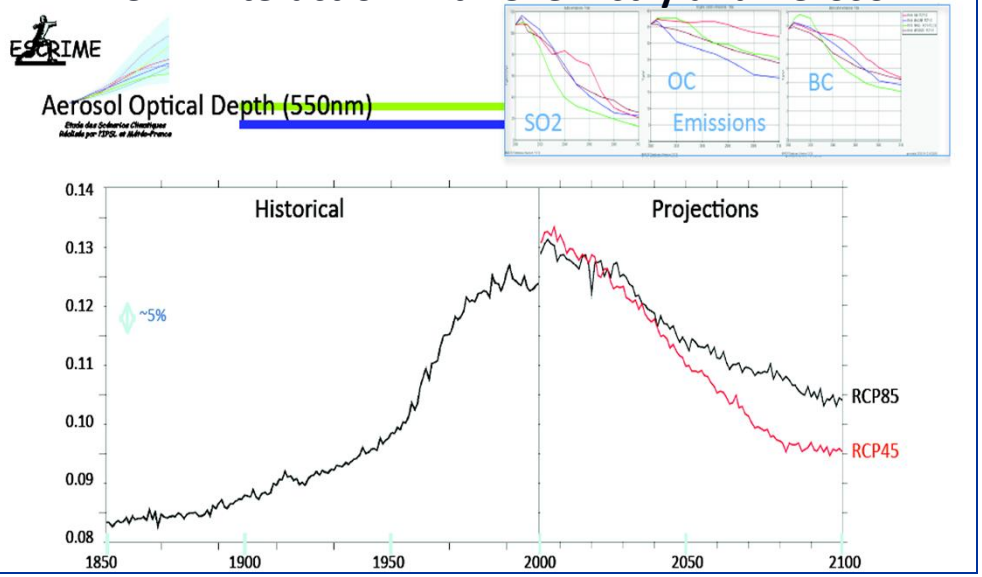

Table 2 Summary of the LMDZ4 experimental design

Expt.	Period	Forcing	Cumulus convection	SST forcing
HIST1	Historical: (1886 – 2005)	Natural and Anthropogenic forcings	Emanuel	SST_ANOM_IPSL_CM5A_HIST + SST_AMIP_CLIM
HISTNAT1	Historical: (1886 - 2005)	Natural only	Emanuel	SST_ANOM_IPSL_CM5A_HISTNAT + SST_AMIP_CLIM
HIST2	Historical: (1950 – 2005)	Natural and Anthropogenic forcings	Tiedtke	SST_ANOM_IPSL_CM5A_HIST + SST_AMIP_CLIM
HISTNAT2	Historical: (1950 – 2005)	Natural only	Tiedtke	SST_ANOM_IPSL_CM5A_HISTNAT + SST_AMIP_CLIM
RCP4.5	Future RCP4.5 scenario (2006 – 2095)	Natural and Anthropogenic forcings	Emanuel	SST_ANOM_IPSL_CM5A_RCP4.5 + SST_AMIP_CLIM
HIST1_GHG	Historical (1950 – 2000) Decadal time slice runs for (1951-1960), (1961-1970), (1971-1980), (1981-1990), (1991-2000)	Natural and GHG-only forcings. Land use and aerosol fields are set to 1886 values	Emanuel	SST_ANOM_IPSL_CM5A_HIST_GHG + SST_AMIP_CLIM
HIST1_PIGHG	Historical: Decadal time slice runs for (1951-1960), (1961-1970), (1971-1980), (1981-1990), (1991-2000)	Includes Natural variations, Aerosol forcing and Land-use change. The concentration of GHGs are set to 1886	Emanuel	SST_ANOM_IPSL_CM5A_HIST + SST_AMIP_CLIM

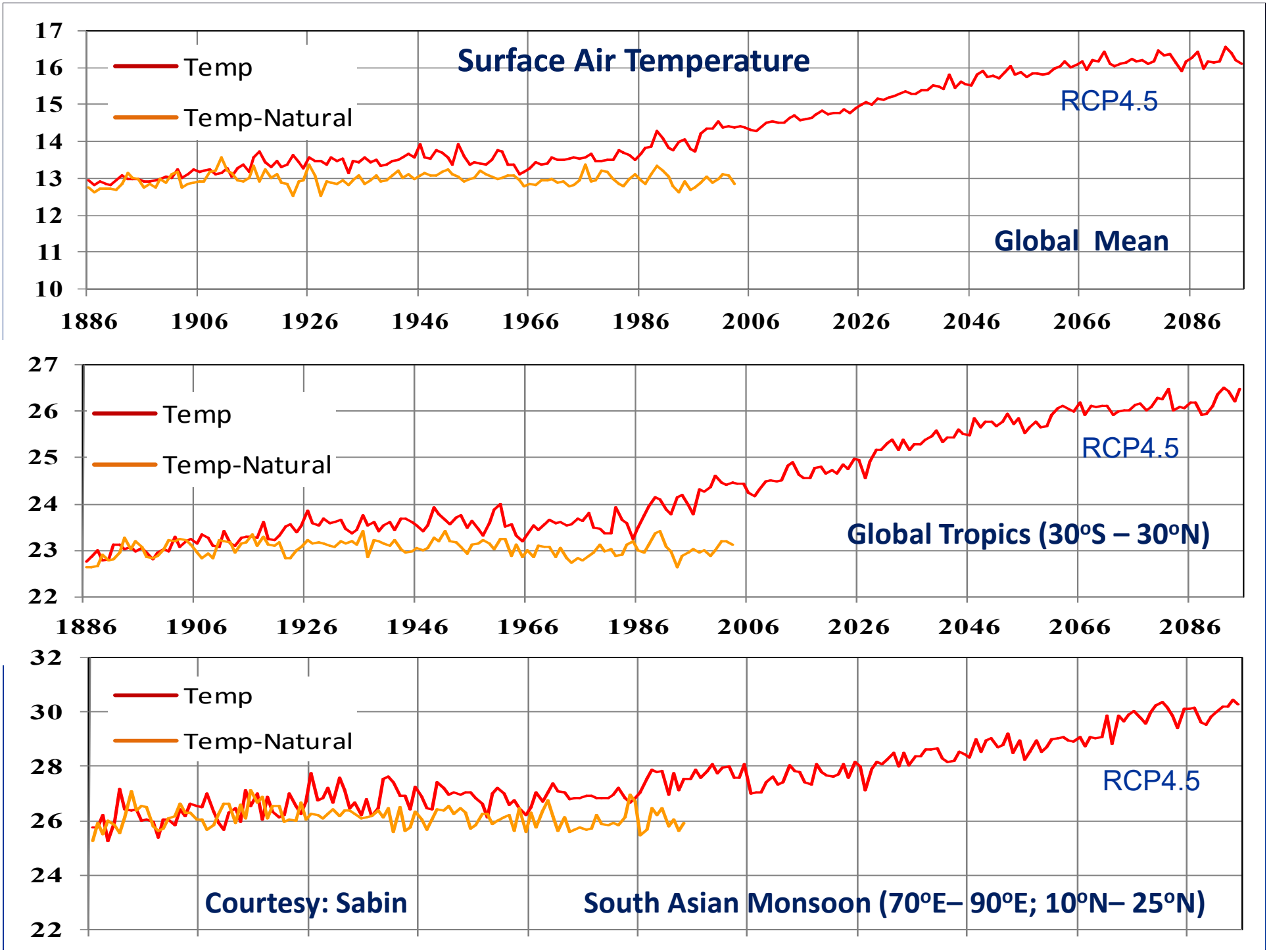
Surface Air Temperature
Temp
Temp-Natural
RCP4.5
Global Mean
17
16
15
14
13
12
11
10
1886
1906
1926
1946
1966
1986
2006
2026
2046
2066
2086
Temp
Temp-Natural
RCP4.5
Global Tropics (30°S – 30°N)
27
26
25
24
23
22
Temp
Temp-Natural
RCP4.5
Courtesy: Sabin
South Asian Monsoon (70°E– 90°E; 10°N– 25°N)
32
30
28
26
24
22

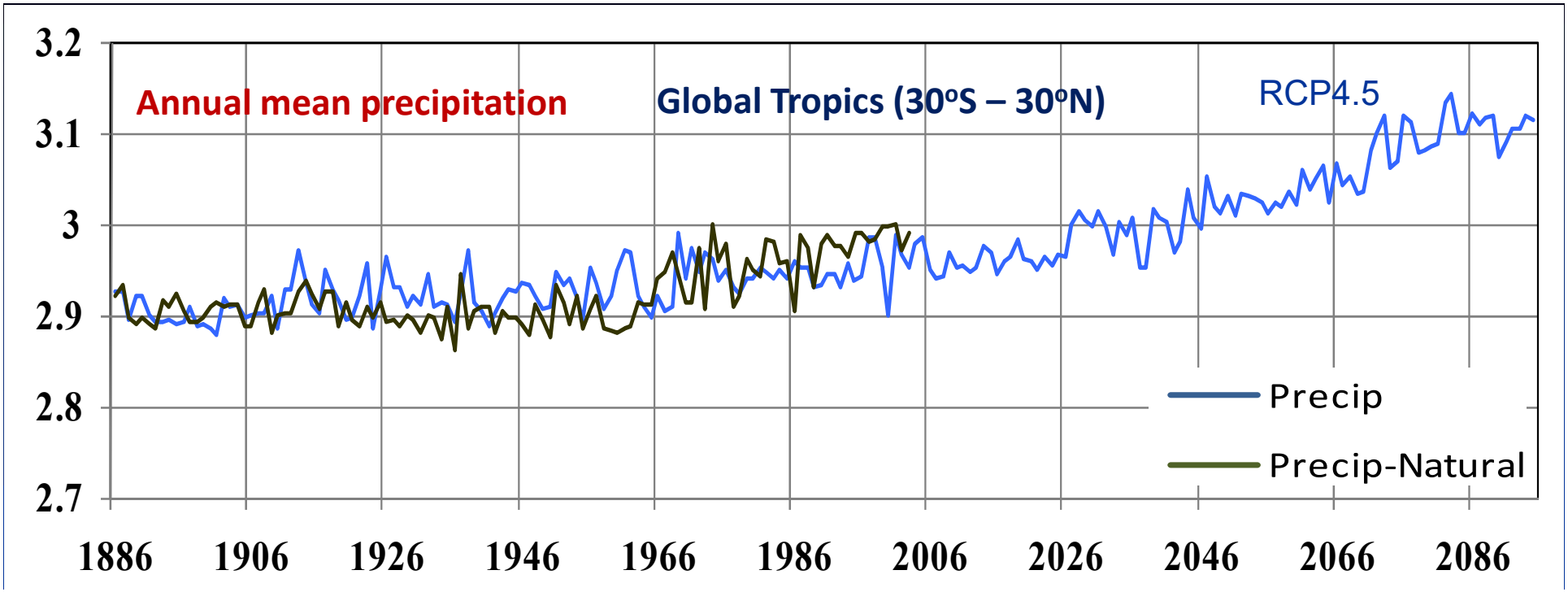
Annual mean precipitation
Global Tropics (30°S – 30°N)
RCP4.5
Precip
Precip-Natural
3.2
3.1
3
2.9
2.8
2.7
1886
1906
1926
1946
1966
1986
2006
2026
2046
2066
2086

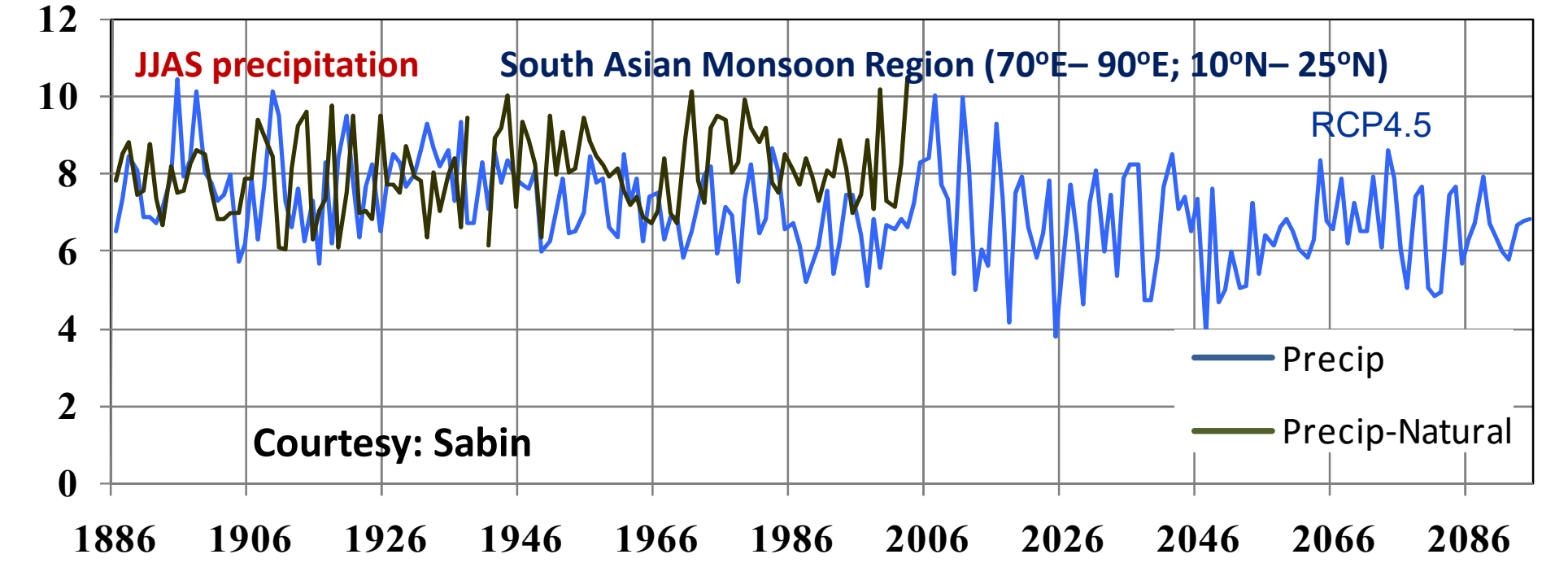
JJAS precipitation
South Asian Monsoon Region (70°E– 90°E; 10°N– 25°N)
RCP4.5
Precip
Precip-Natural
Courtesy: Sabin
12
10
8
6
4
2
0
1886
1906
1926
1946
1966
1986
2006
2026
2046
2066
2086

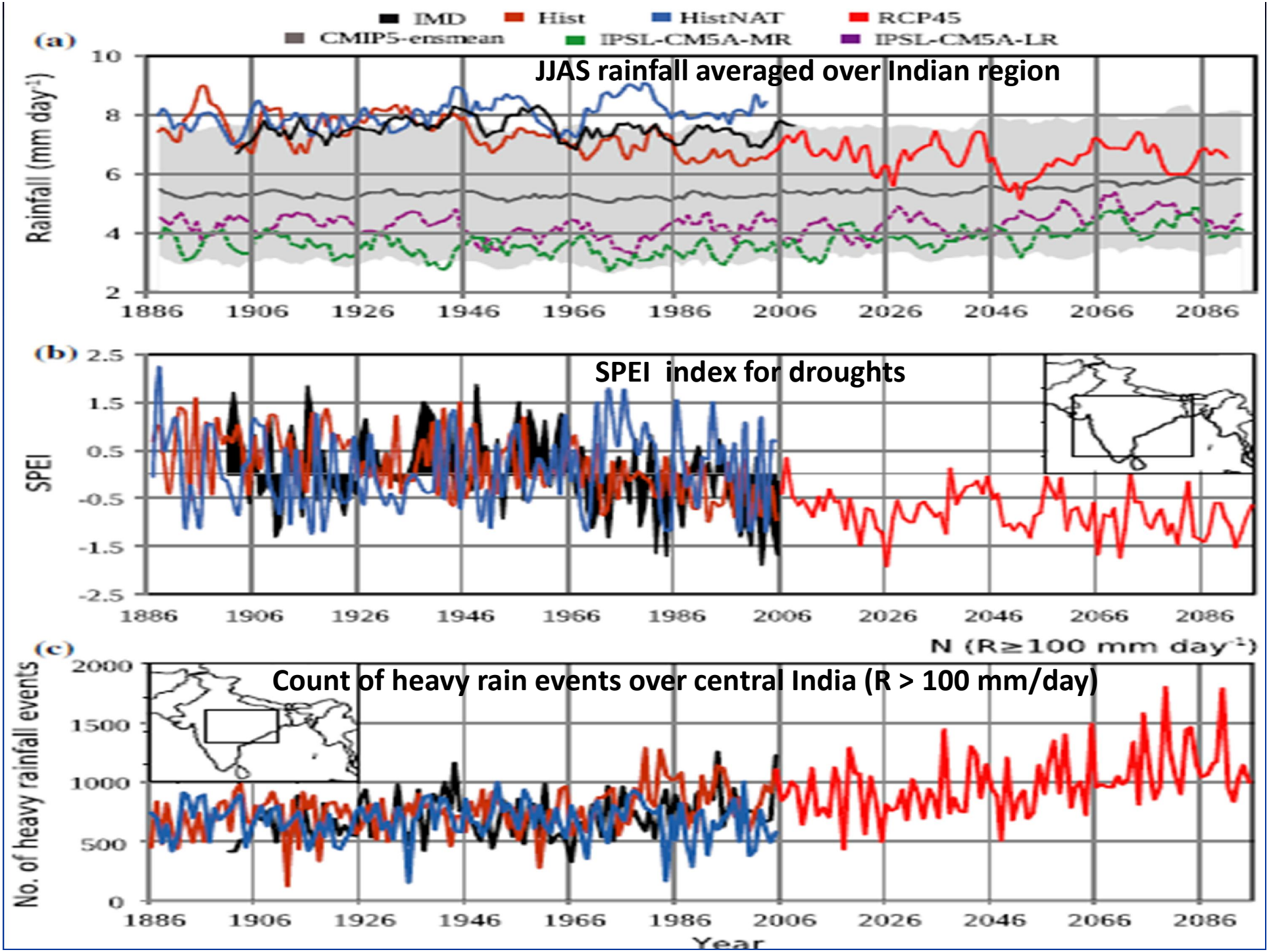
IMD
Hist
HistNAT
RCP45
CMIP5-ensmean
IPSL-CM5A-MR
IPSL-CM5A-LR
(a)
JJAS rainfall averaged over Indian region
Rainfall (mm day-1)
10
8
6
4
2
1886
1906
1926
1946
1966
1986
2006
2026
2046
2066
2086
(b)
SPEI index for droughts
SPEI
2.5
1.5
0.5
-0.5
-1.5
-2.5
N (R≥100 mm day-1)
(c)
Count of heavy rain events over central India (R > 100 mm/day)
No. of heavy rainfall events
2000
1500
1000
500
0
Year

Spatial map of JJAS rainfall trends (1951-2005). Units mm day^{-1} (55 yr)$^{-1}$

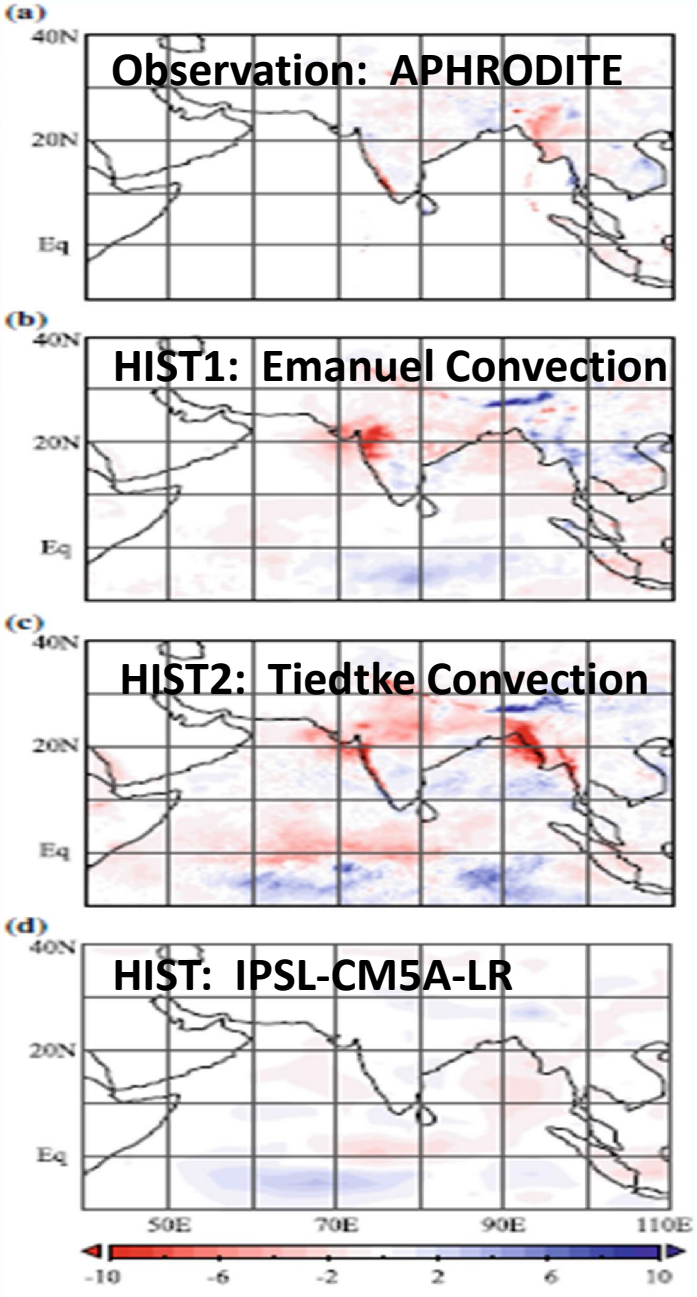

Time-series (1951-2005): JJAS rainfall averaged (70-90E; 10-28N)

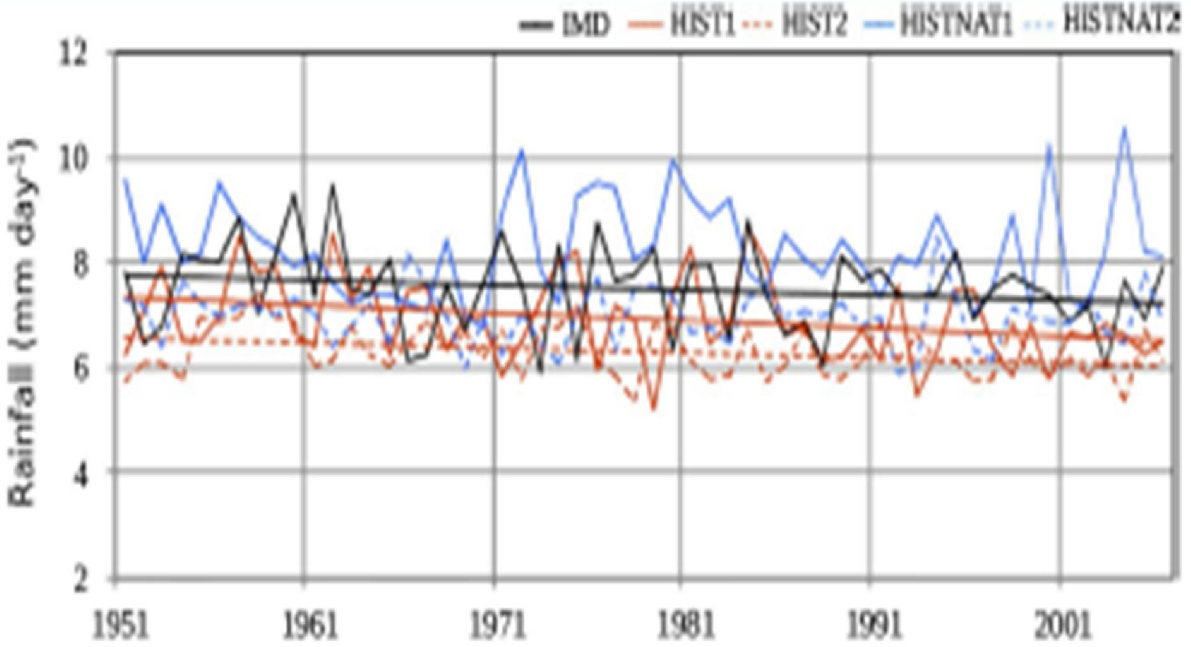

Table 1 Summary of trends of JJAS rainfall averaged over the land points for the Indian region (70°–90°E, 10°–28°N)

	Rainfall trend	Mean rainfall (mm day^{-1})	% change w.r.t mean rainfall	*P* value based on two tailed student's *t* test
IMD dataset (1951–2005)	−0.55 units mm day^{-1} (55 years)$^{-1}$	7.5	−7	<0.01
HIST1 (1951–2005)	−1.1 units mm day^{-1} (55 years)$^{-1}$	6.9	−16	<0.01
HIST2 (1951–2005)	−0.55 units mm day^{-1} (55 years)$^{-1}$	6.3	−9	<0.01
HISTNAT1 (1951–2005)	−0.03 units mm day^{-1} (55 years)$^{-1}$	8.3	−0.3	0.54 (not significant)
HISTNAT2 (1951–2005)	−0.1 units mm day^{-1} (55 years)$^{-1}$	6.9	−1	0.2 (not significant)
RCP4.5 (2006–2060)	−1.1 units mm day^{-1} (55 years)$^{-1}$	6.6	−17	<0.01
RCP4.5 (2006–2095)	−0.29 units mm day^{-1} (90 years)$^{-1}$	6.6	−5	<0.01

Mean difference maps (All-forcing minus Natural) during 1951-2005

JJAS rainfall and 850 hPa winds

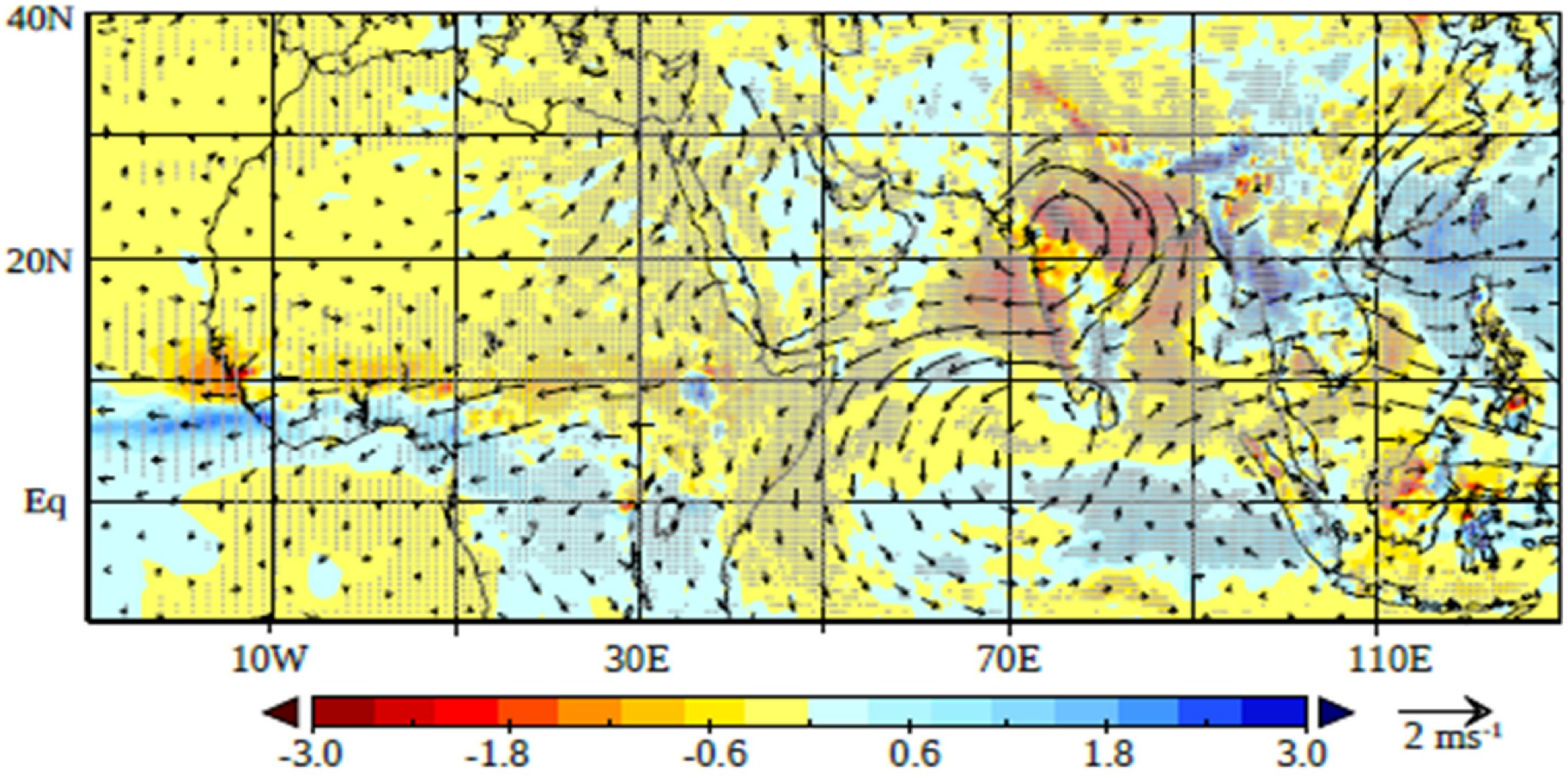

Decomposing the monsoon response to GHG and regional forcing

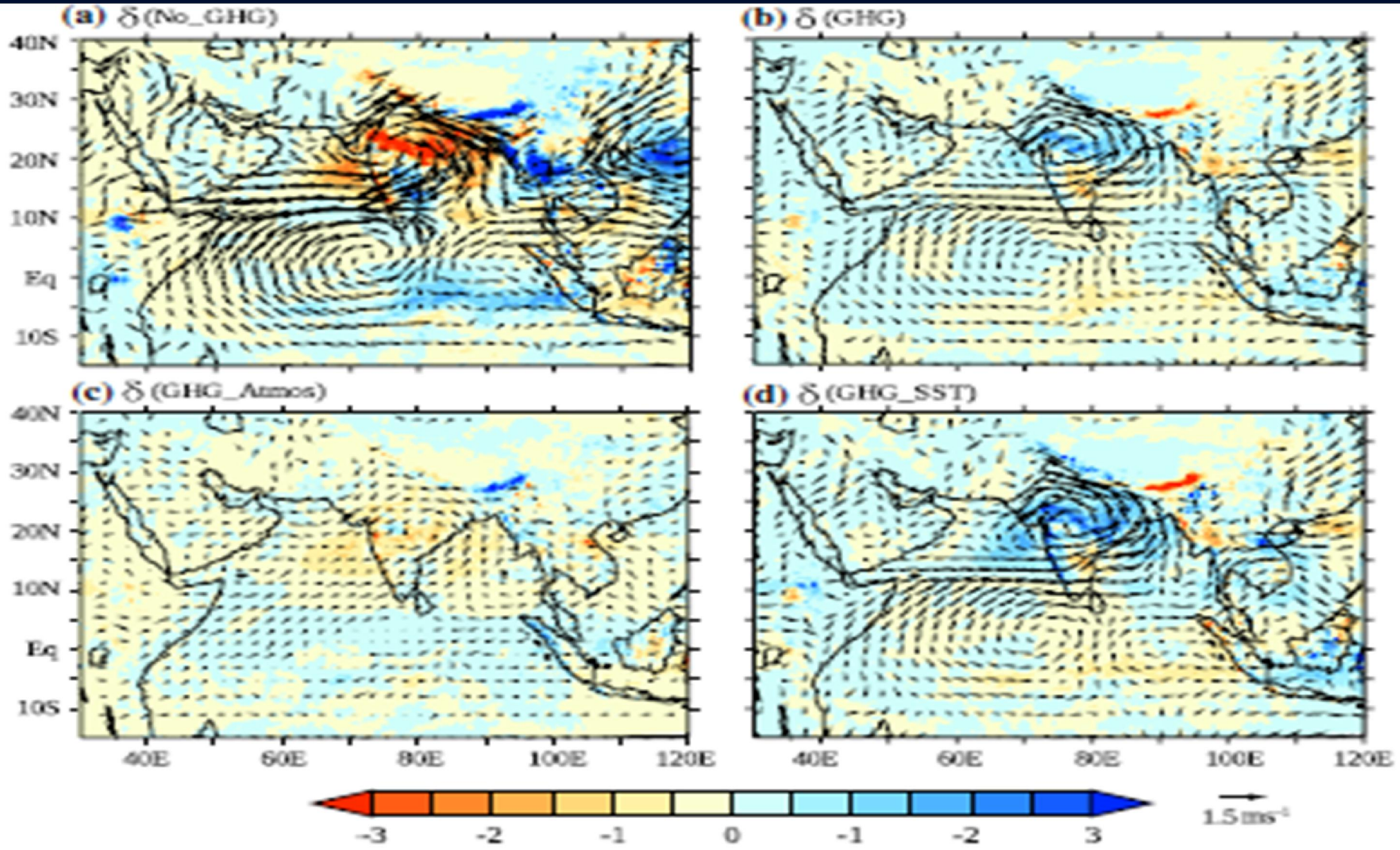

Fig. 6 Decomposing the monsoonal response to GHG and regional forcing elements Composite difference maps of the simulated June–September precipitation (mm day^{-1}) and 850 hPa winds (ms^{-1}), **a** δ(No_GHG) = HIST1 minus HIST1_GHG, **b** δ(GHG) = HIST1_GHG minus HISTNAT1, **c** δ(GHG_Atmos) = HIST1 minus HIST1_PIGHG, **d** δ(GHG_SST) = δ(GHG) minus δ(GHG_Atmos). The composite maps are constructed for the period (1951–2000) using the decadal time-slices

(HIST minus HISTNAT): 1951-2002

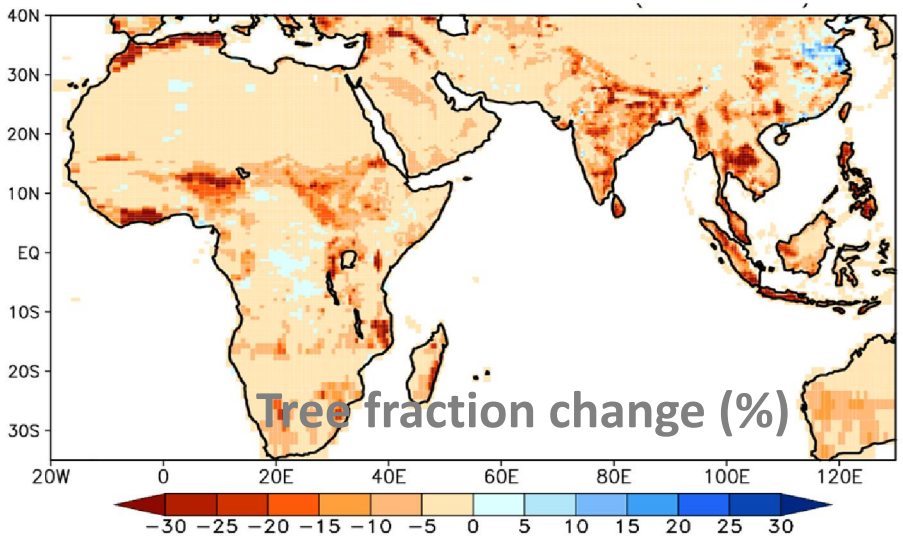

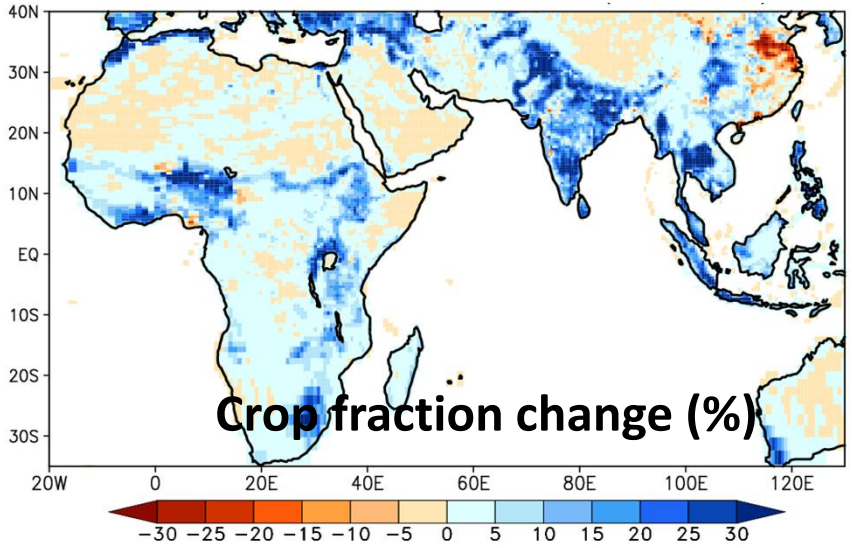

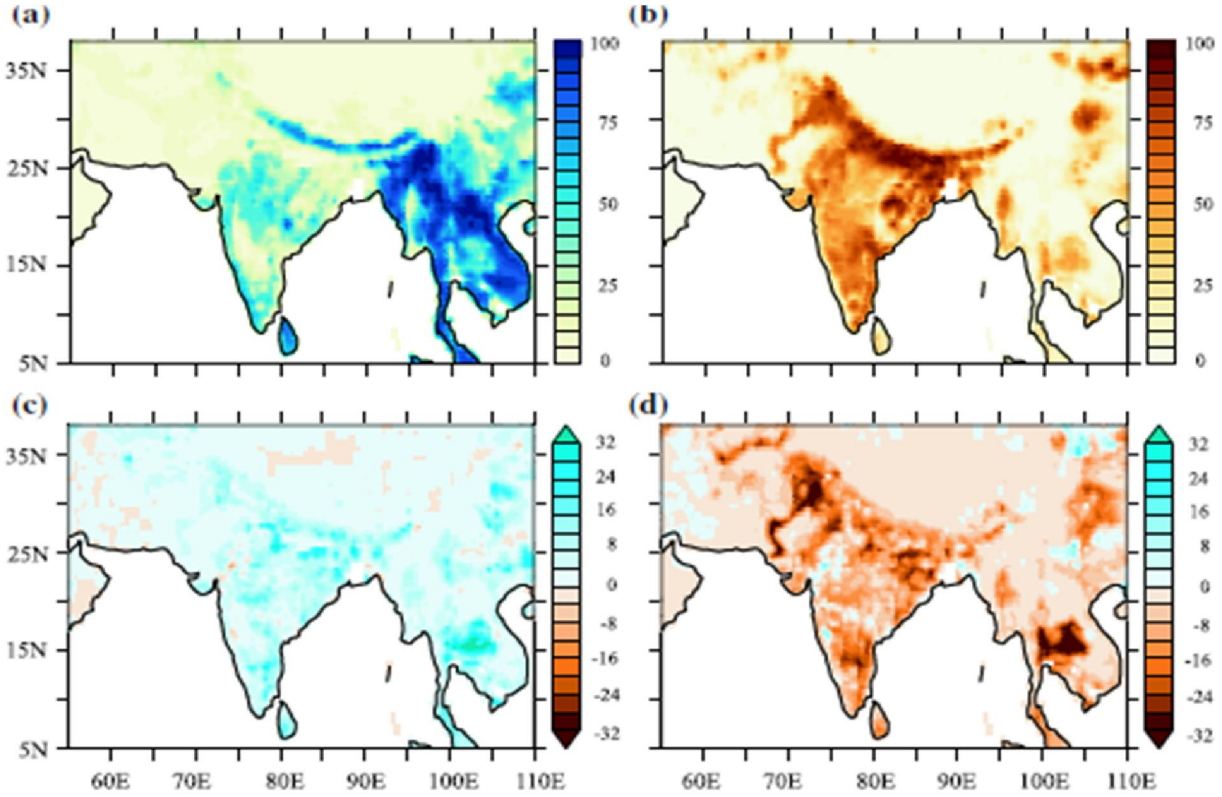

Fig. 8 Spatial maps of land-use used in the LMDZ4 experiments. **a** Mean tree-fraction (%) for the period 1951–2000. **b** Same as **a** except for crop-fraction (%). **c** Change in tree-fraction (%) shown by difference [(1891–1930) minus (1951–2000)] map. **d** Same as **c** except for crop-fraction (%). Note the larger spatial coverage of tree area over South and Southeast Asia and China during (1891–1930) relative to (1951–2000); while the crop area coverage was less during (1891–1930) relative to (1951–2000)

(a) Anthropogenic Aerosol Forcing @ TOA

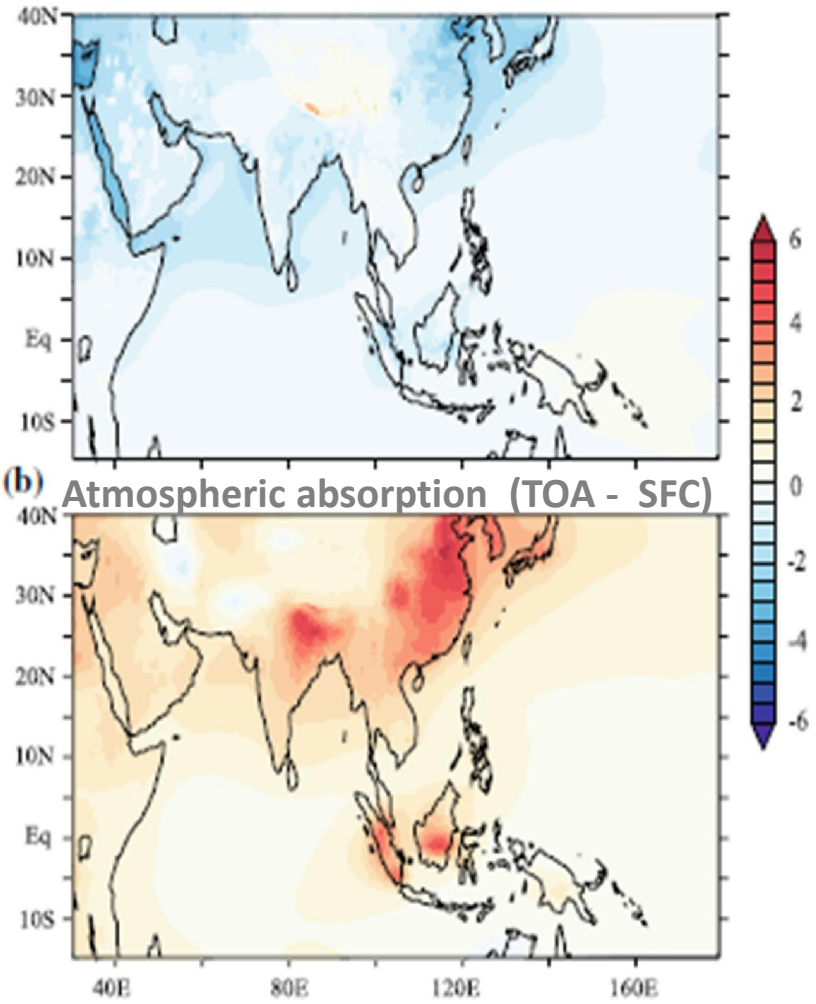

Fig. 9 Spatial distribution of mean anthropogenic aerosol forcing from the HIST1 experiment during 1951–2005. **a** Anthropogenic aerosol forcing (Wm^{-2}) at the top-of-atmosphere (TOA). **b** Atmospheric absorption (Wm^{-2}) due to anthropogenic aerosols (i.e., aerosol-forcing @ TOA minus aerosol-forcing @ Surface). The mean aerosol forcing is computed for the JJAS season from the HIST1 simulation during the period 1951–2005

Map of JJAS SST trend (1951-2005)

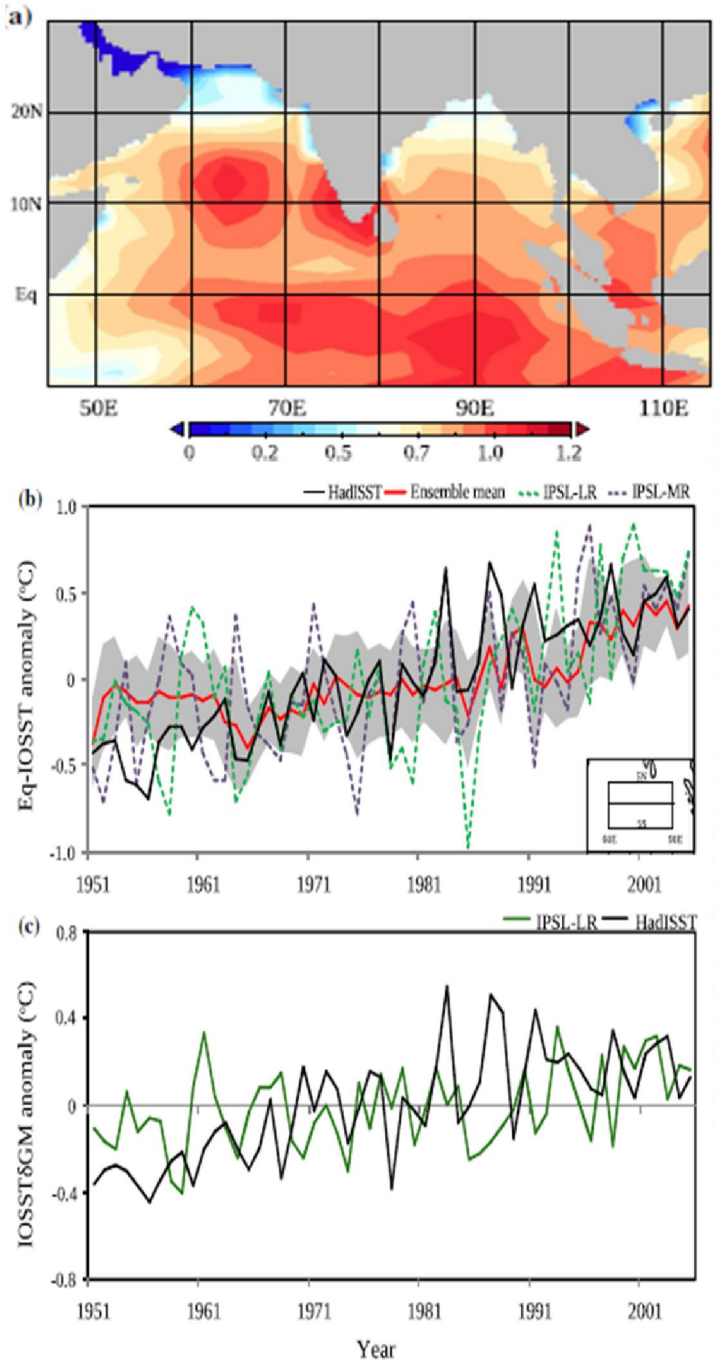

Fig. 10 Tropical Indian Ocean SST warming trend during (1951–2005). **a** Spatial pattern of linear trend of SST (°C per 55 years) from the IPSL-CM5A-LR simulation. **b** Time-series of equatorial Indian Ocean SST (IOSST in °C) anomalies averaged over the region (5°S–5°N, 60°–90°E) from HadISST (*black line*), IPSL-CM5A-LR (*green line*), IPSL-CM5A-MR (*purple*), ensemble mean of CMIP5 models (*red line*). The *grey shading* shows the spread of SST anomalies simulated across the CMIP5 models. **c** Time-series of IOSSTδGM anomalies (°C) (IOSSTδGM = EQIOSST minus Global Mean SST) for HadISST (*black line*), IPSL-CM5A-LR (*green line*). The rapid warming of IOSSTδGM is apparently linked to weakening of the summer–monsoon cross-equatorial flow in recent decades (Swapna et al. 2014)

Long term trends of SST and surface winds over the Tropical Indian Ocean

P. Swapna, R. Krishnan & J. M. Wallace, Climate Dynamics, 2013

June – September (JJAS)

Rest of the year

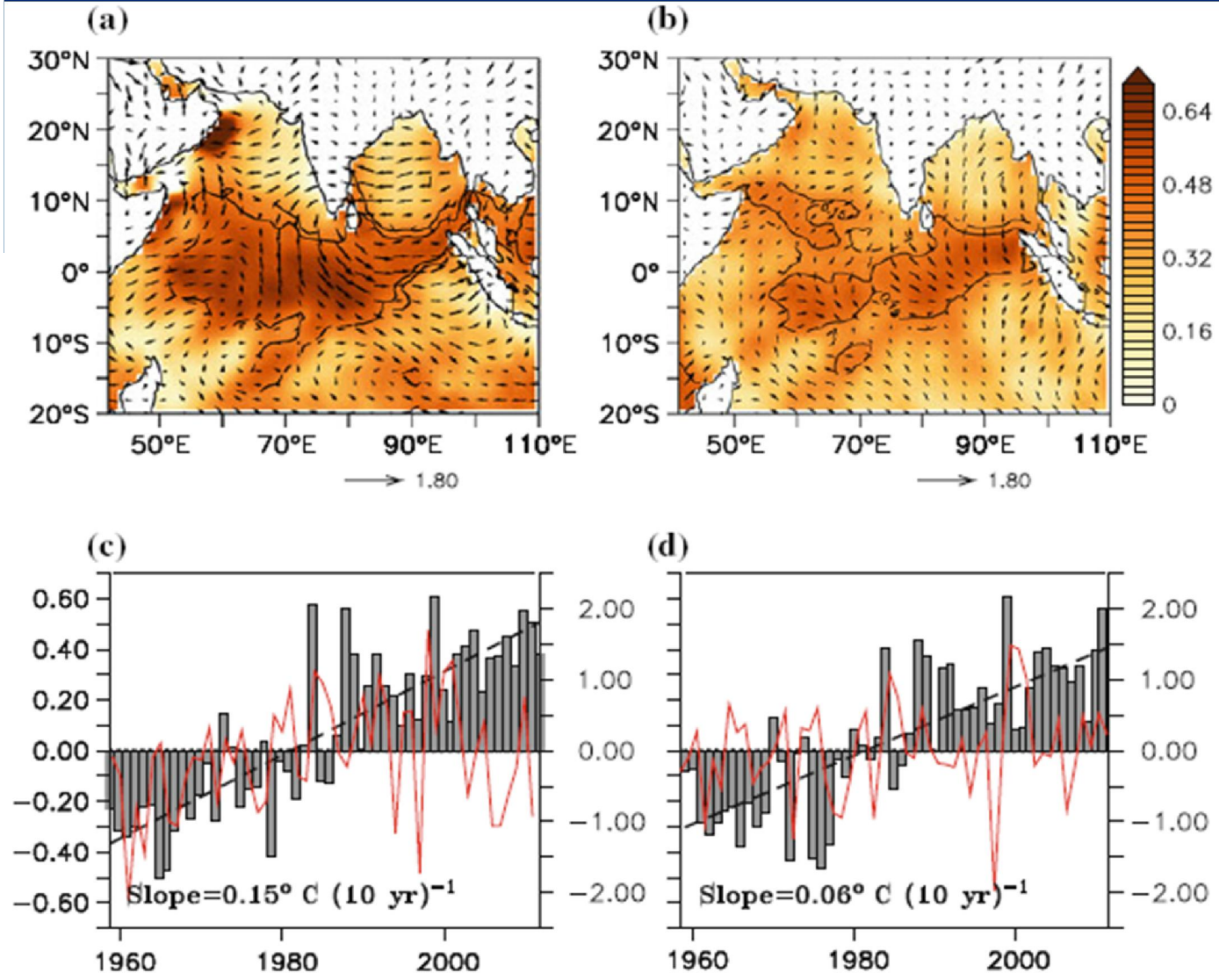

Fig. 1 *Upper panels* show trends in sea surface temperature (SST in °C per 62 years; the departure from the global mean SST) and ERA surface winds (m s^{-1} per 54 years) in the tropical Indian Ocean (IO) for the summer monsoon season. **a** June–September; **b** the remaining calendar months. *Color shading* indicates the magnitude of SST trends and the contour corresponds to 99 % confidence level based on the Student's *t* test (see Balling et al. 1998). The *lower panels* show time-series of SST (°C) bars and ERA zonal wind anomalies (m s^{-1}, *red lines*) averaged over the equatorial IO (50°E–100°E, 5°S–5°N). **c** June–September and **d** the remaining calendar months. The trends of the linear regression best-fit lines exceed the 95 % confidence level

Drying of Indian subcontinent by rapid Indian Ocean warming and a weakening land-sea thermal gradient

Roxy Mathew et al. 2015 Nature Comm.

Mathew Koll Roxy[1], Kapoor Ritika[1,2], Pascal Terray[3,4], Raghu Murtugudde[5], Karumuri Ashok[1,6] & B.N. Goswami[1,7]

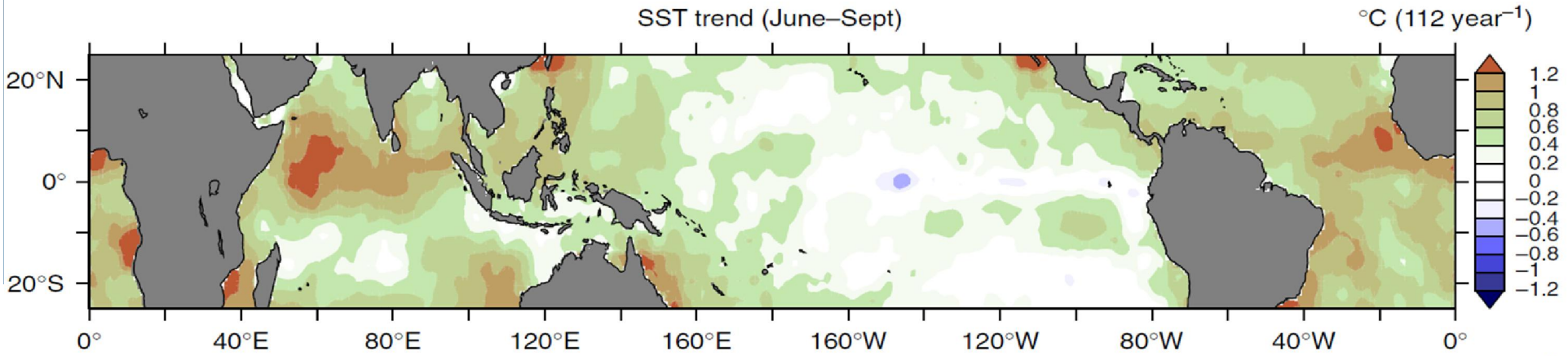

Figure 2 | Summer sea surface temperature trends for the years 1901-2012. Observed trend in mean summer (June-September) SST (°C 112 year^{-1}) over the global tropics during 1901-2012.

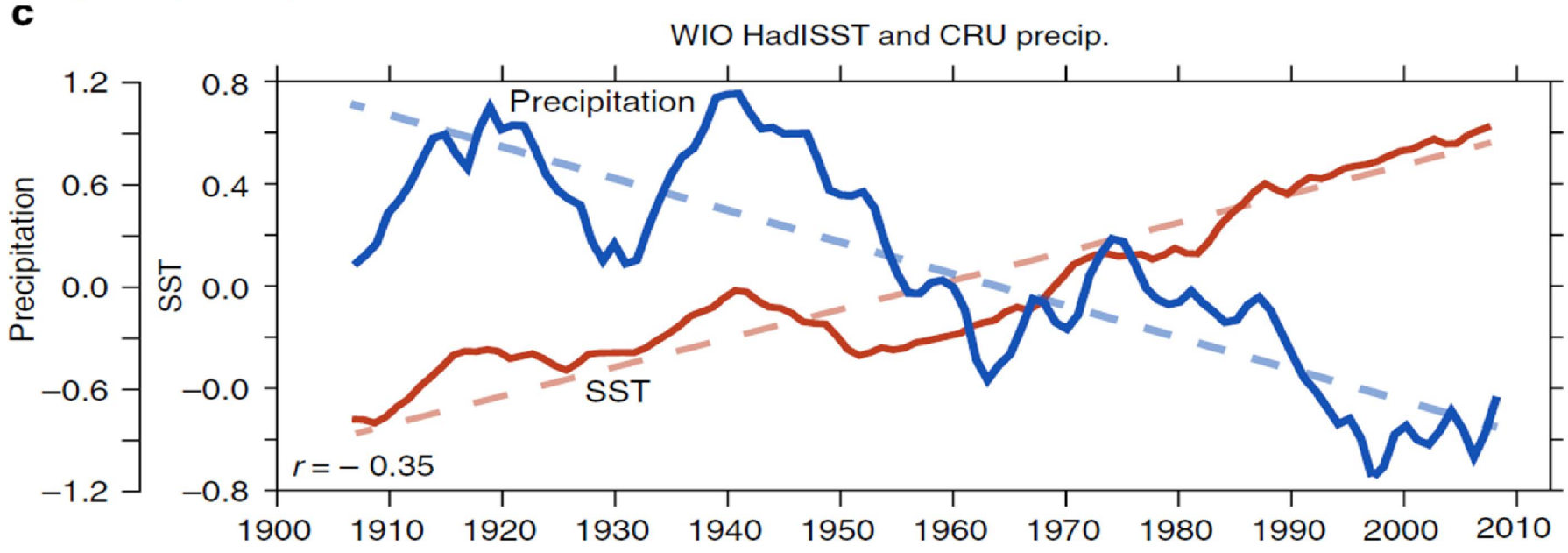

Time-series of regional forcing & simulated response

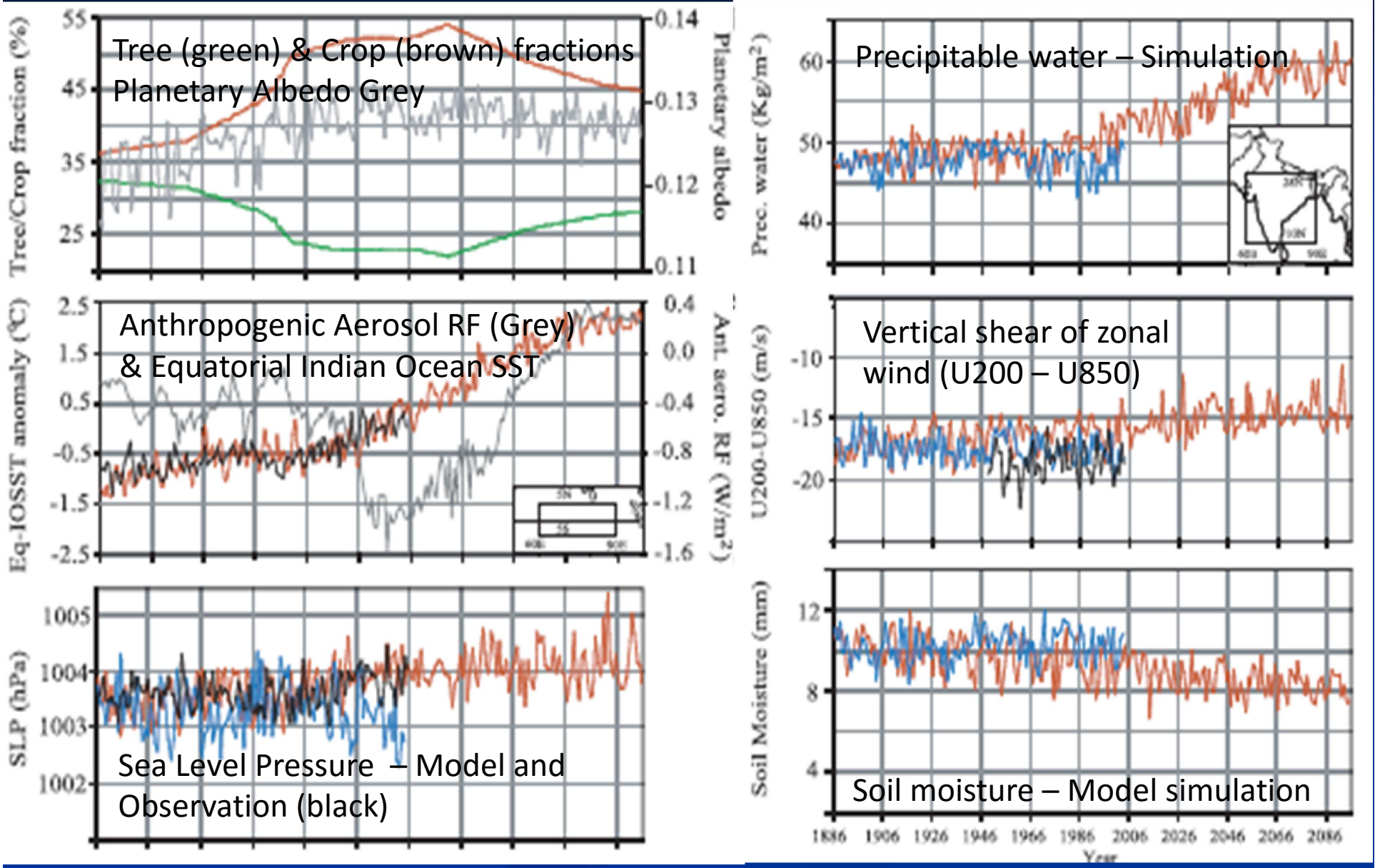

Weakening of monsoon Hadley-type overturning

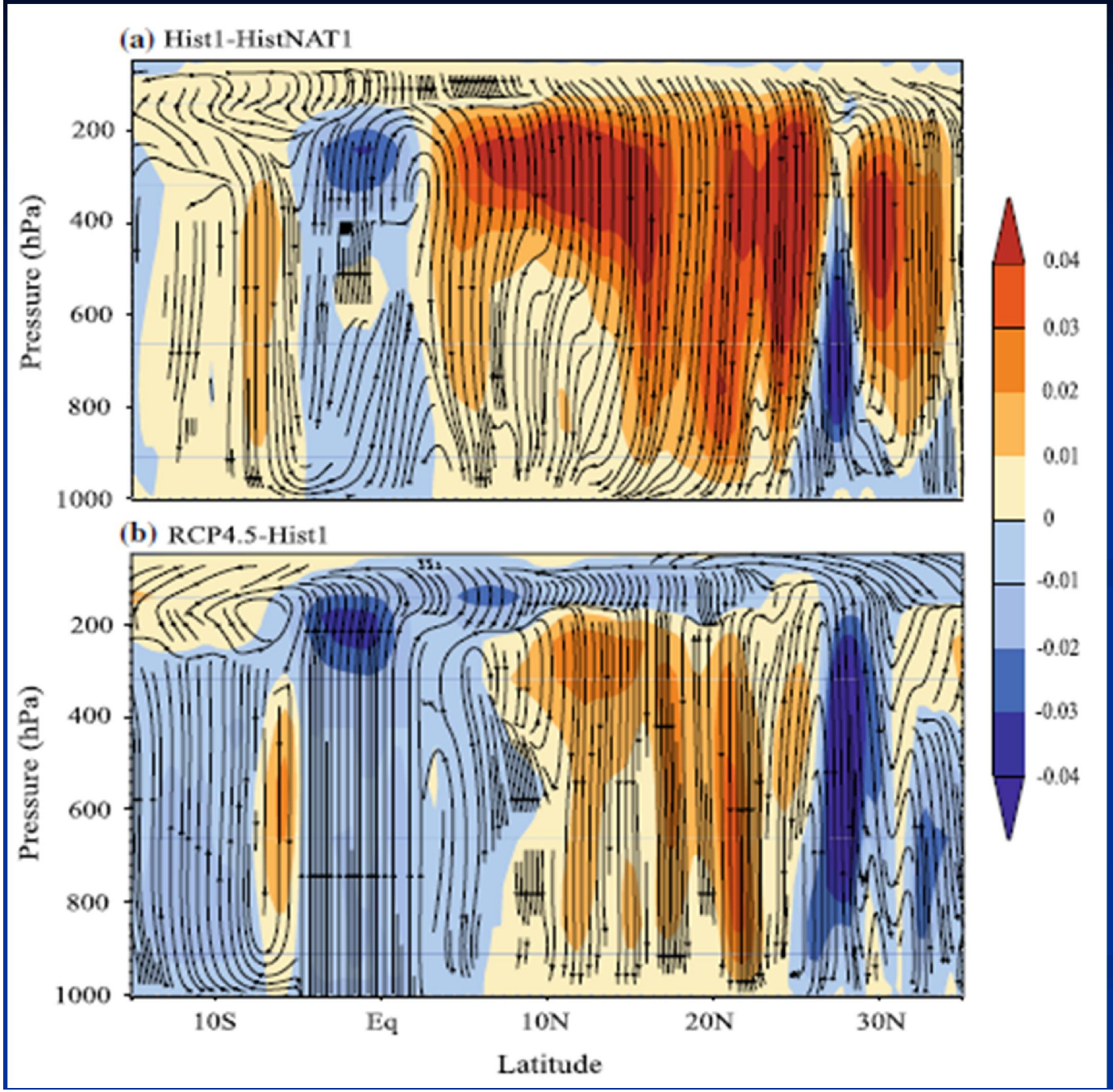

Latitude Pressure sections of difference plots of meridional overturning circulation anomalies

Response of tropospheric temperature & large-scale circulation to Anthropogenic forcing

HIST minus HISTNAT (1951 – 2005): Winds & temperature vertically averaged 600-200 hPa

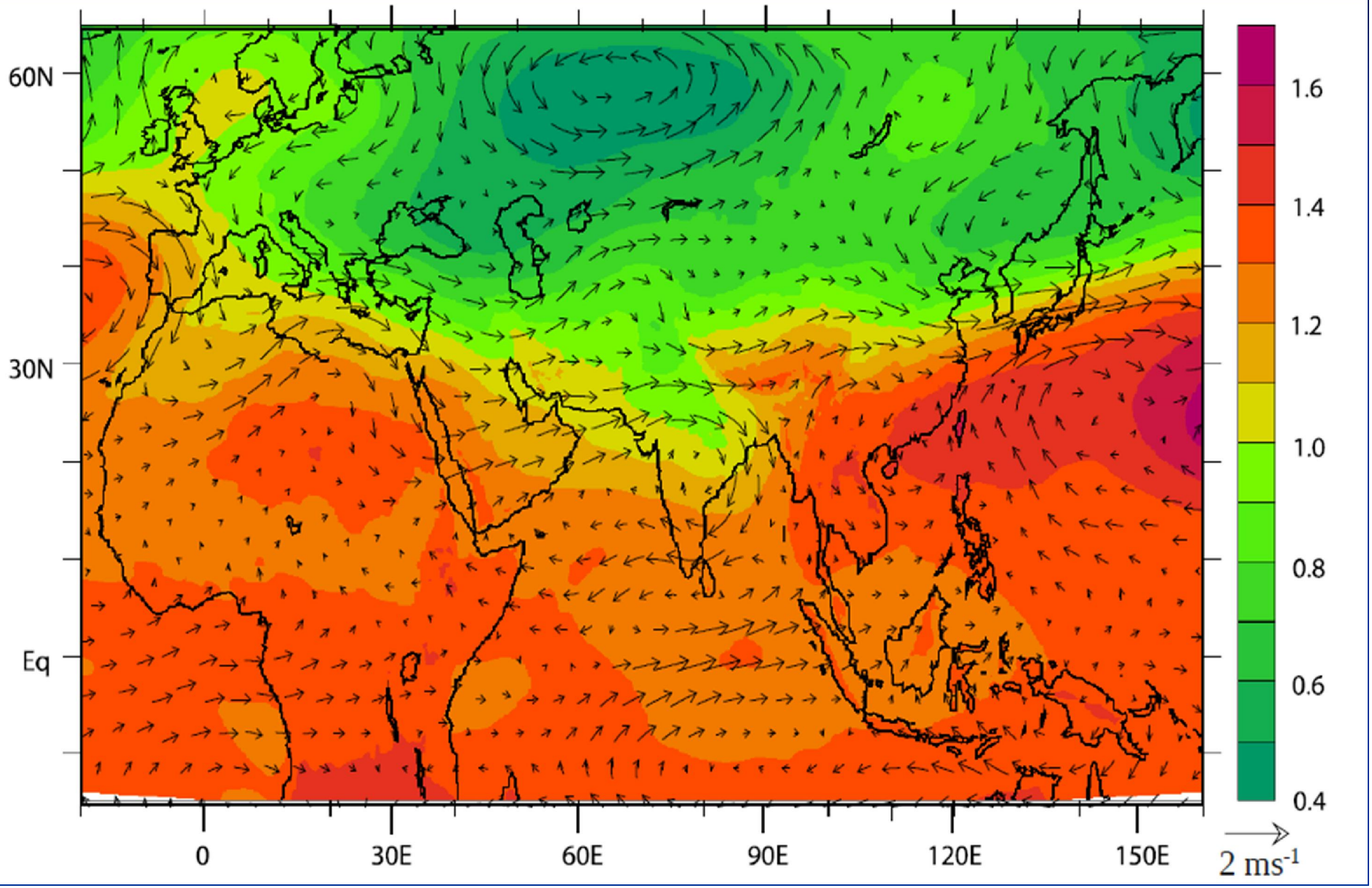

Time-series of year-wise count of heavy rain events (intensity > 100 mm/day) over Central India

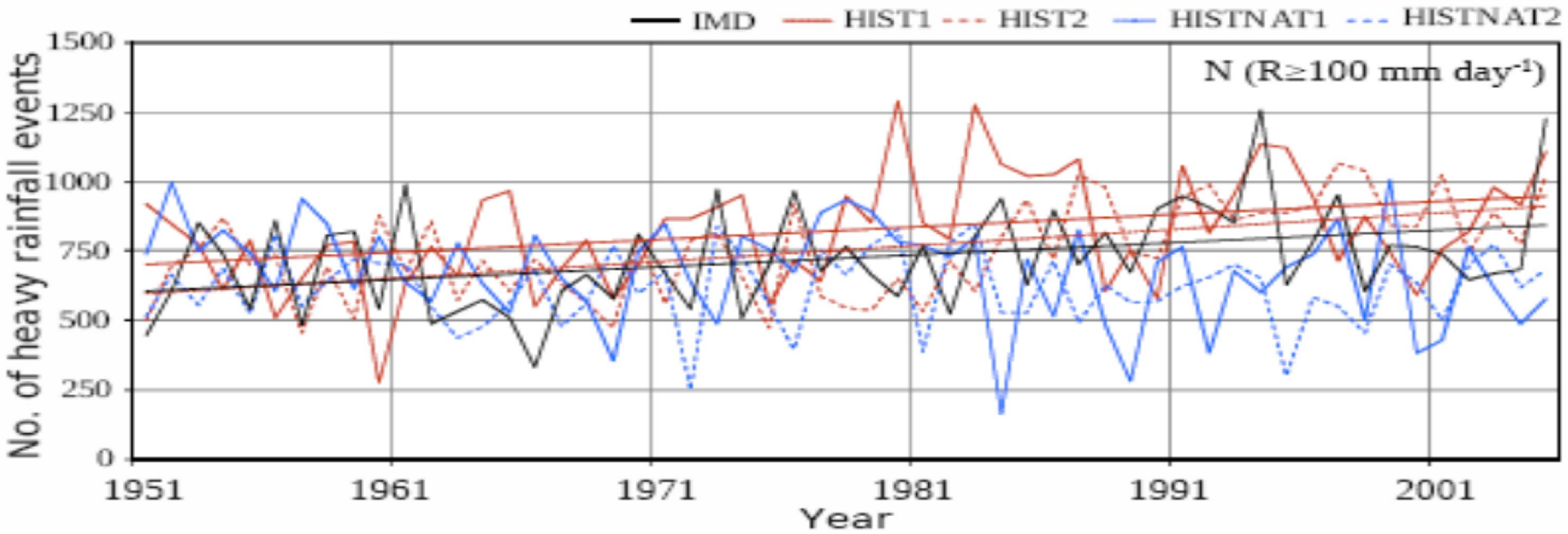

Table 4 Summary of trends in the frequency of heavy precipitation events over Central India, with intensities ≥ 100 mm day^{-1}, from IMD observations and LMDZ4 simulations

	Trend in the frequency count	Mean frequency count	% change w.r.t mean frequency count	*P* value based on the two tailed student's *t* test
IMD dataset (1951–2005)	430 units (55 years)$^{-1}$	1448	30	<0.01
HIST1 (1951–2005)	499 units (55 years)$^{-1}$	1652	30	<0.01
HIST2 (1951–2005)	638 units (55 years)$^{-1}$	1507	42	<0.01
HISTNAT1 (1951–2005)	−34 units (55 years)$^{-1}$	1356	−3	0.2 (not significant)
HISTNAT2 (1951–2005)	+6 units (55 years)$^{-1}$	1233	0.5	0.8 (not significant)
RCP4.5 (2006–2095)	750 units (90 years)$^{-1}$	1976	38	<0.01

Changes in Heavy & Moderate precipitation types to GHG & regional

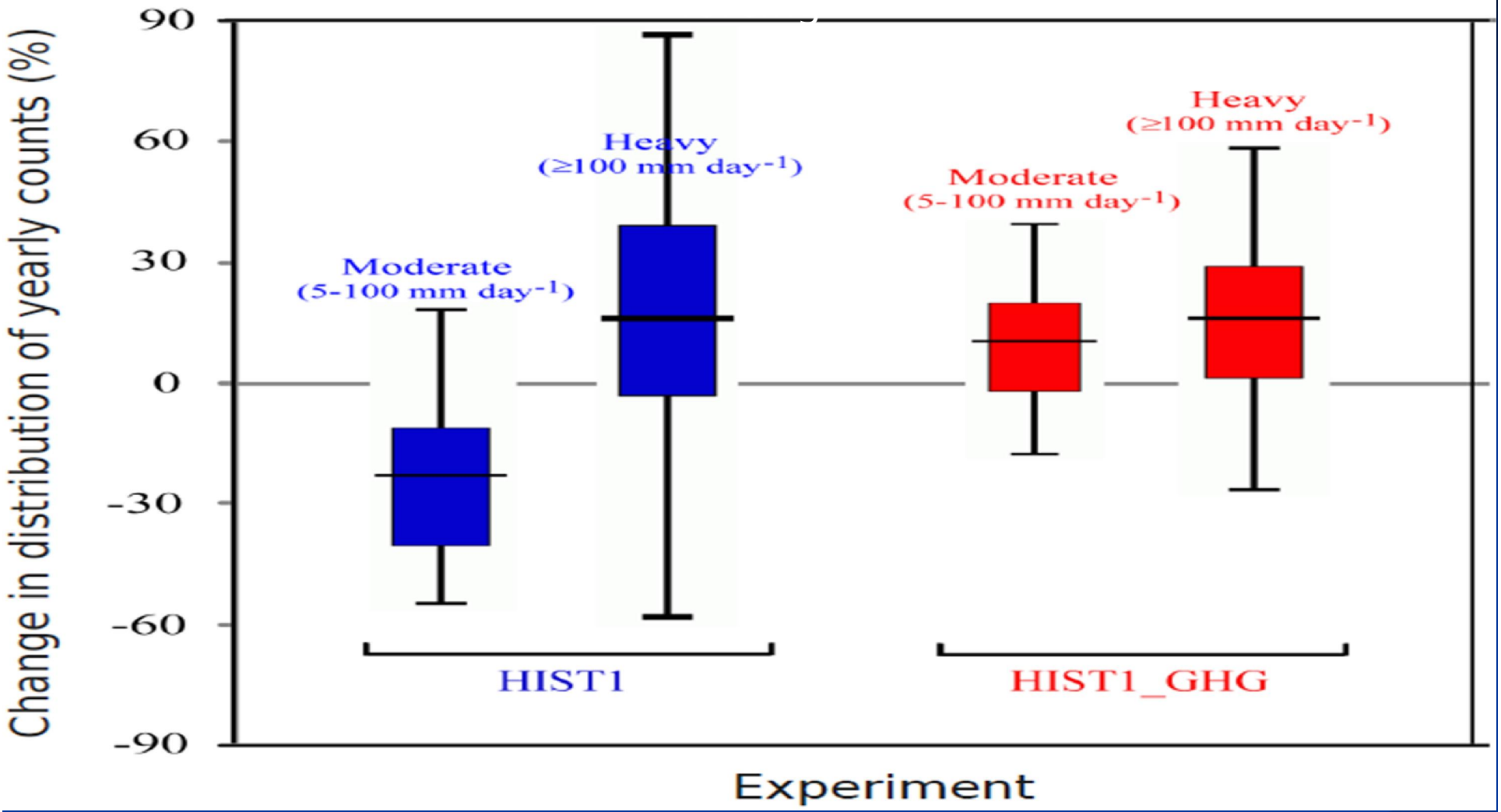

Central India: 74.5°E – 86.5°E, 16.5°N - 26.5°N

Period:1951-2000

Frequency counts for both categories are relative to HISNAT

Summary

•Study of the Indian monsoon in maintaining interactions among different scales (large scale, synoptic system, meso-scale)

•Zoomed version of LMDZ, forced by SST, without lateral boundary condition

•High resolution improves monsoon simulation, both in terms of precipitation and interactions between precipitation and atmospheric circulation – eg., cyclonic systems around monsoon trough. The dry bias of the **NO ZOOM** simulation inhibits moist convective systems and limits westward extension of monsoon precipitation

•Long-term climate change experiments using the high-resolution LMDZ model highlight several value additions as compared to coarse resolution simulations

•The high-resolution simulation with anthropogenic forcing captures the decreasing trend of Indian monsoon precipitation in the post-1950s . Recent monsoon decline is likely influenced by regional forcing elements (ie., anthropogenic aerosols, land use and land cover change, equatorial Indian Ocean warming

•Robust increase in frequency of heavy precipitation (R > 100 mm/day) occurrences over Central India is noted in the high-resolution climate change simulation

Limitations of the present study

- Absence of atmosphere-ocean coupling in stand-alone atmospheric GCMs is a limitation for studying the South Asian monsoon coupled system

- Strong internal variability of the South Asian monsoon system

- Single realization for HIST1 (Emanuel Convection) and HIST2 (Tiedtke Convection)

- Separating the effects of aerosol forcing and land-use change ?

- Indian Ocean Warming Signal (decadal variability and long-term trend): Not adequately understood

- Way Forward ?

THE IITM EARTH SYSTEM MODEL

Transformation of a Seasonal Prediction Model to a Long-Term Climate Model

BY P. SWAPNA, M. K. ROXY, K. APARNA, K. KULKARNI, A. G. PRAJEESH, K. ASHOK, R. KRISHNAN, S. MOORTHI, A. KUMAR, AND B. N. GOSWAMI

This work documents the fidelity of the newly developed Indian Institute of Tropical Meteorology climate model simulations and demonstrates its suitability to address the climate variability and change issues relevant to the South Asian monsoon.

IITM-ESM - Radiatively balanced system. Realistic global climate. Mean monsoon rainfall & interannual variability captured

ENSO-Monsoon tele-connections and PDO - Pacific Decadal Oscillation are robust

Improvements in sea-ice and Atlantic THC

Time-varying aerosol properties and land-use land cover to be used for CMIP6

Interactive Ocean Biogeochemistry

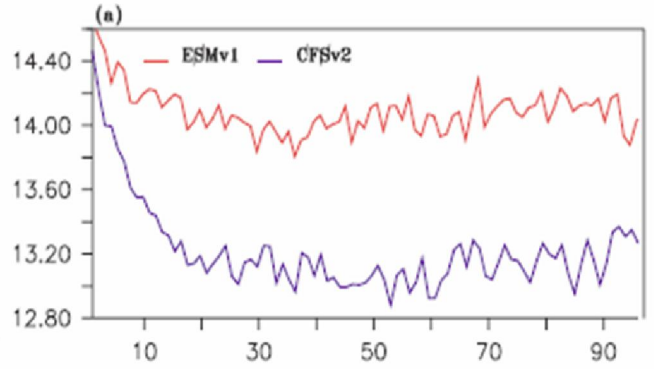

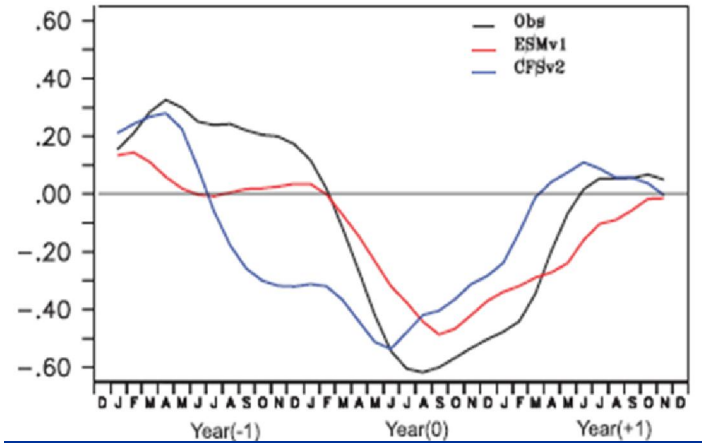

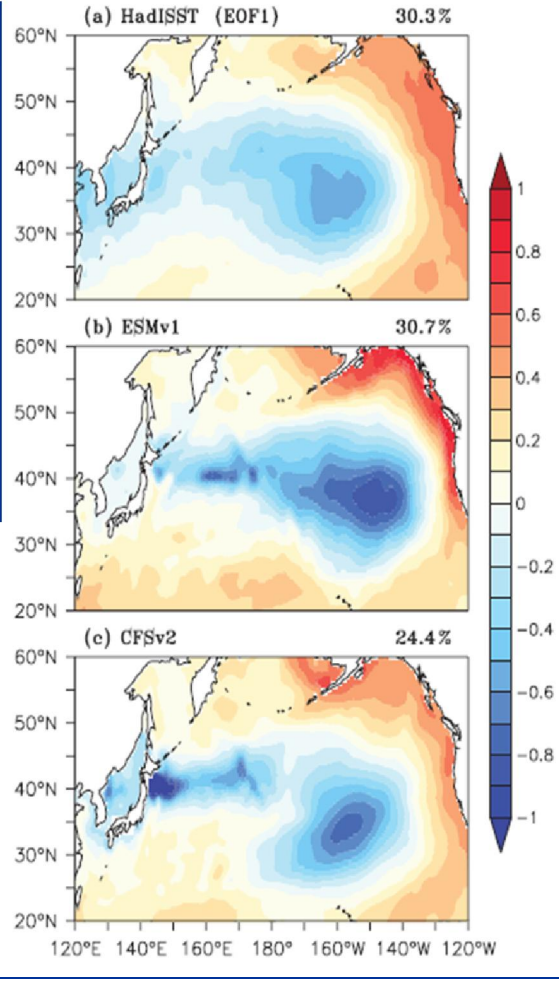

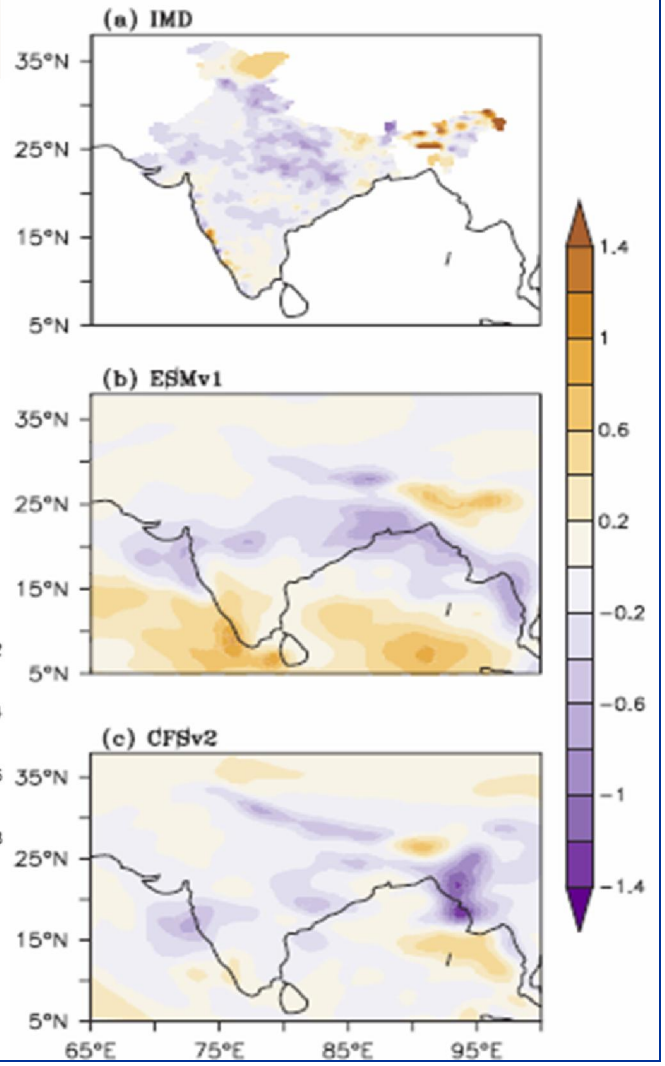

Thank you